Remote Sens. **2011**, *3*, 2494-2528; doi:10.3390/rs3112494

OPEN ACCESS

Remote Sensing

ISSN 2072-4292

www.mdpi.com/journal/remotesensing

Article

Airborne Light Detection and Ranging (LiDAR) for Individual Tree Stem Location, Height, and Biomass Measurements

Curtis Edson and Michael G. Wing *

Department of Forest Engineering, Resources, and Management, Oregon State University, Peavy Hall 204, Corvallis, OR 97331, USA; E-Mail: curtis.edson@oregonstate.edu

* Author to whom correspondence should be addressed; E-Mail: michael.wing@oregonstate.edu; Tel.: +1-541-737-4009; Fax: +1-541-737-4316.

Received: 28 September 2011; in revised form: 20 October 2011 / Accepted: 20 October 2011 / Published: 18 November 2011

Abstract: Light Detection and Ranging (LiDAR) remote sensing has demonstrated potential in measuring forest biomass. We assessed the ability of LiDAR to accurately estimate forest total above ground biomass (TAGB) on an individual stem basis in a conifer forest in the US Pacific Northwest region using three different computer software programs and compared results to field measurements. Software programs included FUSION, TreeVaW, and watershed segmentation. To assess the accuracy of LiDAR TAGB estimation, stem counts and heights were analyzed. Differences between actual tree locations and LiDAR-derived tree locations using FUSION, TreeVaW, and watershed segmentation were 2.05 m (SD 1.67), 2.19 m (SD 1.83), and 2.31 m (SD 1.94), respectively, in forested plots. Tree height differences from field measured heights for FUSION, TreeVaW, and watershed segmentation were −0.09 m (SD 2.43), 0.28 m (SD 1.86), and 0.22 m (2.45) in forested plots; and 0.56 m (SD 1.07 m), 0.28 m (SD 1.69 m), and 1.17 m (SD 0.68 m), respectively, in a plot containing young conifers. The TAGB comparisons included feature totals per plot, mean biomass per feature by plot, and total biomass by plot for each extraction method. Overall, LiDAR TAGB estimations resulted in FUSION and TreeVaW underestimating by 25 and 31% respectively, and watershed segmentation overestimating by approximately 10%. LiDAR TAGB underestimation occurred in 66% and overestimation occurred in 34% of the plot comparisons.

Keywords: LiDAR; biomass; forestry; inventory

1. Introduction

Forest attribute inventory information and measurements are critical to forest management [1]. Historically, forest inventories have focused on timber production [2] but recent inventories have concentrated on fuel biomass and carbon stores due to interest in bioenergy and carbon sequestration and concerns over global climate change [3-5]. A significant problem in monitoring carbon stores in vegetation biomass is the persistent deficiency of accurate biomass estimates [6].

Biomass is the measurement of plant material mass per unit area. Biomass measurement is sometimes limited to living plant material, but based on the slow deterioration of woody vegetation; the measurement sometimes includes dead material. Above ground biomass is the "mass of live or dead organic matter" [6]. The unit of measure is commonly g/m^2 or kg/ha. Biomass is measured via four primary means: (a) *in situ* destructive measurement; (b) *in situ* non-destructive using equations or conversion; (c) derived from remote sensing; and (d) modeling [4,6]. Allometric equations are used to statistically infer biomass based on *in situ* field data or remotely sensed data for extrapolation to larger land areas. Allometry assumes that a relationship exists by species based on structural measurements, usually height and stem or base diameter [6].

Light Detection and Ranging (LiDAR) has recently emerged as significant technology for forest measurement applications. Forest measurements derived from LiDAR include ground and vegetation surfaces, which are used to assess tree height, volume, and biomass measurements [7]. Many forest attributes can be measured by LiDAR over large areas including canopy height, subcanopy topography, vertical canopy distribution [8], and individual tree heights [9]. Tree height measurement is a critical component of forest inventory measurements [9,10]. When measuring tree heights using LiDAR, accuracy is impacted by several factors including size and reflectivity of the tree, shape of the tree crown, and LiDAR pulse density and footprint (pulse diameter). A primary source of error in LiDAR tree height measurement associated with conifer species occurs when laser pulses miss the sharp apex of the tree resulting in an underestimation of tree height [11,12]. Discrete returns from LiDAR pulses that strike the canopy may be used to estimate tree heights, or canopy elevations may be derived from a canopy height model (CHM) [13]. A CHM is raster surface model, similar to a digital elevation model (DEM), interpolated from points acquired on the upper surface of the canopy. Based on the tree structure, errors in LiDAR tree height measurement are also dependent on the algorithm used to create the CHM [2]. LiDAR tree height estimates are calculated by subtracting the terrain surface as represented by DEM from the highest point associated with an individual tree [8,14].

Several key measurements are required to accurately estimate stand height, stem and forest volume, basal area, stem density, biomass [15], carbon sequestration, growth and site productivity [9]. Husch *et al.* [10] describe the most common forest measurements of stem diameter, crown diameter and height. The standard US diameter measurement is diameter at breast height (DBH), which is measured at 1.3 m above the ground on the uphill side and 1.4 m when trees are located on level ground. Crown diameter may be used as a predictor variable for determining DBH and therefore used to estimate tree volume. Tree height may also be used to estimate DBH based on allometric equations [4]. The crown is defined as "the part of the tree or woody plant bearing live branches and foliage". Crown cover (*synonym* canopy cover) is defined as "the ground area covered by the crowns of trees or woody vegetation as delimited by the vertical projection of crown perimeters and commonly expressed as a percent of total ground area" [16]. One of the critical measurements in forest mensuration for determining volume or mass is tree height [9]. Stem volume estimation has traditionally been based exclusively on DBH, but estimates combining height and DBH have proven more accurate if the heights are measured with little or no bias [13,17]. Husch [10] defines three different tree heights that are important to consider in forest measurements including total height, bole height, and merchantable height. These are especially important in considering tree heights measured by LiDAR. Total height is "the distance along the axis of the tree stem between the ground and the tip of the tree"; bole height is "the distance along the axis of the tree stem between the ground and the crown point (crown point is the position of the first crown-forming branch)"; merchantable height is the "distance along the axis of the tree stem between the ground and the terminal position of the last usable portion of the tree stem". These measurements are often summarized and presented as stand level averages.

Much of the focus on LiDAR research has been on trees occupying a dominant and co-dominant portion of the canopy. Some may consider the necessity of a young-tree inventory as not important or less important than established stands, especially considering a priori knowledge resulting from near term management operations. However, monitoring the status of young stands with trees of under 10 m in height is important for growth projections. In addition, stem density is important in planning thinning or planting treatments [18]. Understory vegetation including shrubs and young trees can amount to large amounts of biomass, which is important for estimating carbon stores and monitoring fuels for fire risk mitigation. Thus, this research not only focuses on LiDAR forest mensuration capabilities in dominant and co-dominant canopies, but also in the suppressed sub-canopy. In other words, what vegetation can discrete return LiDAR detect, and what does it miss? Previous research suggests that LiDAR pulses do not strike as much of the suppressed sub-canopy vegetation compared to the dominant and co-dominant canopy and that these suppressed points are not used in generating the CHM [2-4,19-21]. We are not only interested in the accuracy of LiDAR in measuring detected trees, but we also seek to quantify the woody vegetation that is missed by LiDAR on an individual tree and area volume basis. Our study has four primary objectives related to measuring forest tree and shrub features.

Our first objective was to determine the characteristics of individual trees and shrubs that LiDAR detects and misses within a range of forest settings. We believe this is not only a function of tree and shrub size, but is also influenced by the horizontal and vertical density of vegetation and tree species (deciduous or coniferous). The second objective was to determine the accuracy of LiDAR tree and shrub height measurements of detected features compared to ground measured heights. The third objective was to determine the horizontal x and y location accuracy of LiDAR measured trees and shrubs. The fourth objective was to compare hectare volume estimates derived from LiDAR data to ground measured estimates. We evaluated our study objectives with three different techniques for delineating individual tree and shrub measurements: inverse watershed segmentation, TreeVaW, and FUSION.

Inverse watershed segmentation, henceforth referred to as watershed segmentation, is the most common method applied to determining locations of individual tree crowns using a CHM by segmenting the inverted raster canopy surface into the equivalent of individual hydrologic drainage basins [22,23]. Following inversion, a watershed segmentation algorithm separates the CHM into distinct tree polygons with raster crown diameter and height values [24].

TreeVaW operates on a CHM using a variable window filter (VWF) that varies its search window size [1,25], otherwise known as a convolution kernel [26], by passing a local maxima (LM) filter over the CHM and determines a tree location based on elevation data contained in individual pixels [1]. Surrounding pixels are assumed to represent laser hits of the same tree crown, and the highest elevation value is taken to indicate the tree apex [27]. When the filter determines a LM value, a tree x and y coordinate location is identified and then the crown diameter is determined based on the allometric relationship to height [25,27].

The Silviculture and Forest Models Team of the United States Department of Agriculture (USDA) Forest Service, Pacific Northwest Research Station in conjunction with the University of Washington Precision Forestry Cooperative has developed a data management and visualization software tool named "FUSION" that is designed specifically for analyzing forest vegetation characteristics using LiDAR data. The program is capable of generating both DEM and CHM surface models, intensity images from the raw LiDAR point files, and analyzing XYZ point data clouds on a plot basis. After identifying a tree, the user manually measures its dimensions using a three-dimensional cylinder measurement marker. The cylindrical measurement marker is capable of measuring a feature's horizontal coordinate location, height, crown width, and crown height [28].

2. Materials and Methods

2.1. Study Site

The study was conducted in Oregon State University's (OSU) 5,475 ha McDonald-Dunn research forest ranging in elevation from approximately 75–660 m above sea level in the eastern foothills of the Oregon Coast Range in the USA (Figure 1). Conifers dominate the forest with Douglas-fir (*Pseudotsuga* menziesii) and grand fir (*Abies grandis*) being the apex species. The primary deciduous tree species is bigleaf maple (*Acer macrophyllum*) and shrub species California hazel (*Corylus cornuta var. california*).

Figure 1. McDonald-Dunn Forest and surrounding communities within Oregon, USA.

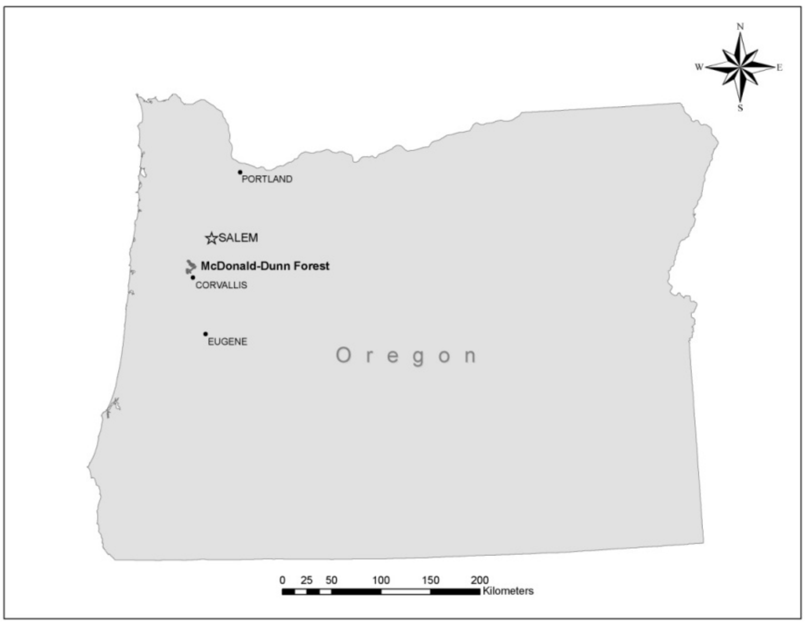

Eleven total plots, one ha (10,000 m^2) in size, were sampled with plot strata consisting of either old growth/mature (referred to as old growth in this study) (two plots), even-aged (two plots), uneven-aged (three plots), or clearcut (four plots) treatments. Plots were selected by stratified random sampling (Table 1). Plot naming corresponds to the silviculture treatment (C = clearcut; E = even-age; O = old growth; and U = uneven-age) and GIS grid number used for random selection.

Table 1. Plot statistics for tree and shrub measurement comparison. Total station measurements collected on five plots and GPS measurements collected on all plots.

Plot	C20	C27	C61	C110	E200	E412	O16	O69	U8	U13	U56
Slope Aspect	NW	NW	NE	NE	E	NE	NE	N	E	SE	NE
Slope Degree	24	18	13	9	7	14	17	28	17	14	8
Slope Percent	45	32	22	16	13	25	31	55	32	25	14
GPS											
Tree Count	691	565	534	575	946	929	363	238	192	498	1255
Shrub Count	8	15	0	118	56	57	140	-	-	47	72
Total Station											
Tree Count	N/A				910	N/A	355	257	367	385	N/A
Shrub Count					78		173	45	153	48	
LiDAR Feature Count	825	647	632	619	1067	957	210	222	191	311	824
Percent Crown Cover	11	9	10	9	65	27	47	46	43	38	70
* Stand Age yrs.	6	6	6	6	21	13	156	138	85	94	57

* Stand age in years based on oldest trees in the stand at time of LiDAR acquisition. Shrubs were not counted by GPS survey crews on plots O69 and U8. The N/A refers to plots not measured using the total station survey instrument.

The most represented conifer species within the study plots was Douglas-fir (*Pseudotsuga menziesii*) (Table 2) with a large contingent of grand fir (*Abies grandis*) in the uneven-aged and old growth plots (Figure 2). Ponderosa pine (*Pinus* ponderosa) and Pacific yew (*Taxus brevifolia*) were found in limited circumstances in addition to several other isolated individuals such as silver fir (*Abies alba*) and western hemlock (*Tsuga heterophylla*). Although the forest is dominated by conifers, the primary deciduous tree species occupying the subcanopy is bigleaf maple (*Acer* macrophyllum). Many other broadleaf tree species were inventoried including cascara buckthorn (*Rhamnus* purshiana), cherry (*Prunus sp.*), and ocean spray (*Holodiscus discolor*) (33 in plot O69) and many others typical of the region in far fewer numbers. California hazel (*Corylus cornuta*) is prolific in this region and dominated the understory species of all plots except clearcut where it had obviously been managed. Besides bigleaf maple, many other isolated shrubs typical of the region were inventoried, and ocean spray was conspicuous in two plots. The densest ground cover was found on C110, which had portions covered in Oregon grape (*Berberis nervosa*) and poison oak (*Rhus diversiloba*) (not inventoried). The discrepancy between GPS and total station in tree counts for Plots U8 and U13 (Table 1) may be explained by two reasons. In Plot U8, the GPS measurements were made for a separate project where only trees 3 m tall and larger were measured. In Plot U13, several small trees on the cusp of the measurement criteria appear to have been overlooked by the total station survey crew.

Figure 2. Plot locations in McDonald-Dunn Forest.

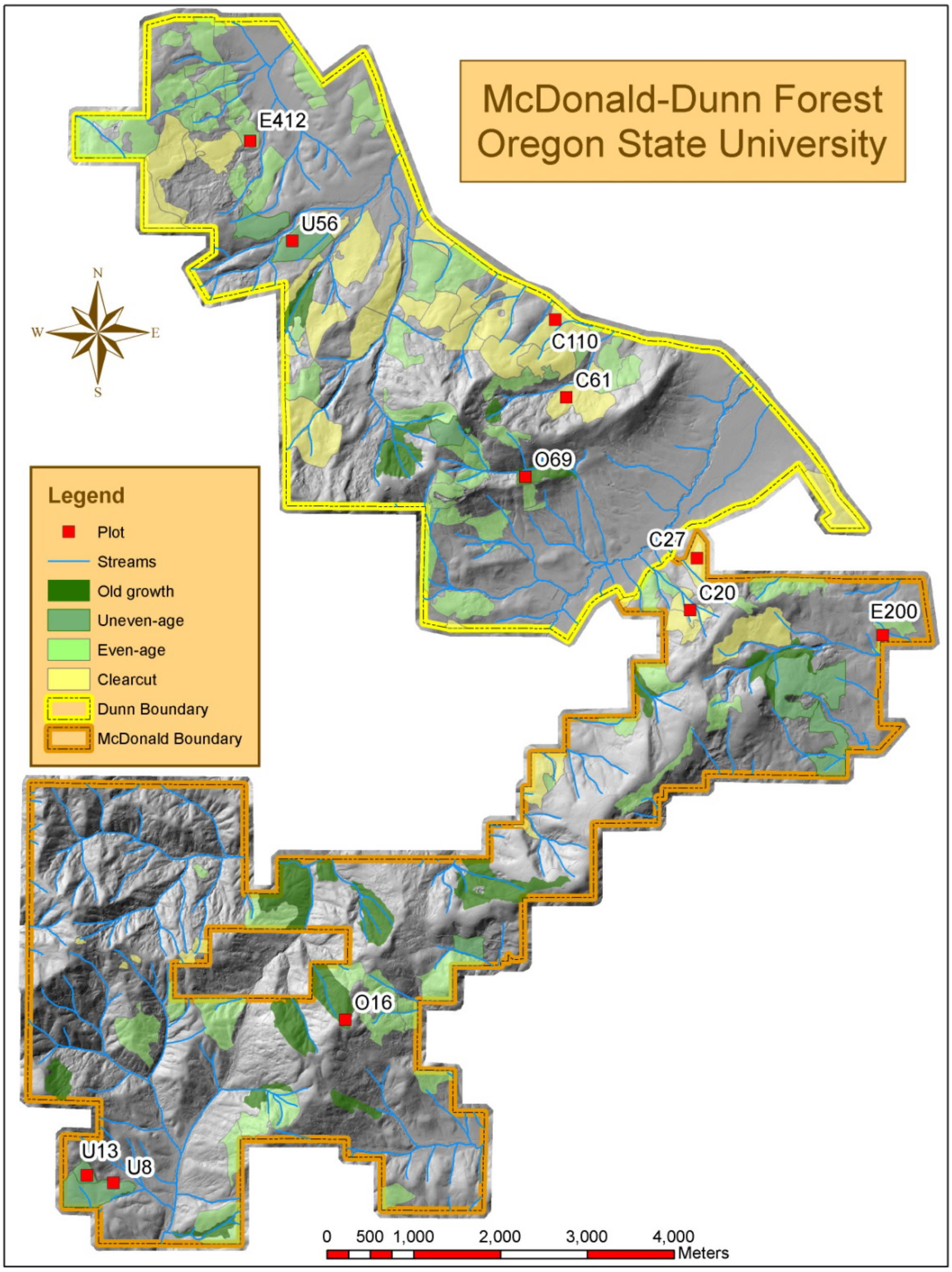

2.2. Tree and Shrub Measurements

The field data collected for trees were species, height, crown width, DBH for stem diameters 13 cm and larger, diameter at ground level (DBA) for stem diameters under 13 cm for all trees one meter and taller (0.61 m and taller in clearcut plots) (Table 2). Heights for tall trees were measured using an Impulse 200LR laser range finder. Height poles were used to measure trees shorter than three meters and all shrubs. A diameter tape was used for DBH and a caliper for DBA. Crown radii for large trees were measured using a range finder and measuring the distance between the projection of the crown vertically to the ground and the tree stem. Small trees and shrub crown measurements were made using a tape measure. In all cases two crown measurements were made per feature. The first length was measured at the longest stem in the crown, and the second was taken at 90° around the stem in a clockwise direction. The crown diameter was then estimated by averaging the two crown measurements, multiplying by two, and adding the DBH. Canopy base height was measured using the FUSION software program as it was not measured by field crews.

Table 2. Study total tree and shrub counts by species common name.

All Trees	Count	Conifers Only	Count	All Shrubs	Count
SPECIES		SPECIES		SPECIES	
bigleaf maple	371	Douglas-fir	5,245	Bigleaf maple	110
California hazel	8	grand fir	876	California hazel	381
cascara buckthorn	76	pacific yew	20	Cascara buckthorn	2
cherry	247	Pacific silver fir	8	cherry	17
cottonwood	1	ponderosa pine	49	Douglas-fir	1
Douglas-fir	5,245	Total	6,198	holly	9
grand fir	876			madrone	1
hawthorne	6	Conifers Minus Snags		mountain mahogany	1
holly	6	SPECIES		oceanspray	73
madrone	10	Douglas-fir	5,156	Oregon white oak	5
oceanspray	3	grand fir	866	Oregongrape	64
Oregon white oak	9	Pacific yew	20	Pacific dogwood	6
Oregongrape	9	Pacific silver fir	8	red elderberry	12
Pacific yew	20	Ponderosa pine	48	Scoular's willow	2
Pacific dogwood	2			snowberry	1
Pacific silver fir	8	Total	6,098	vine maple	12
ponderosa pine	49			other	14
red elderberry	6				
vine maple	10			Total	711
other	18				
Total	6,980				

2.3. Total Station Survey

A Nikon DTM 310 total station with a rated angular accuracy of five-seconds was used to collect the coordinate locations for trees and shrubs in five of the eleven plots. All trees at 1 m and greater in height and all shrubs with a crown diameter of 1 m and greater were measured. Tree sweep was measured for conifer trees that had a noticeable lean angle, thus indicating a different tree apex location compared to its base. Tree coordinate data collected using the total station involved sighting on a rod-person who was positioned directly at the tree stem for small trees or using a two meter rod-measured offset for large trees. The offset distance error was periodically verified using a metric tape and resulted in a mean error of 0.07 m (SD = 0.07). Coordinates, species, health, dbh, and height of all trees and shrubs were determined and recorded.

Survey control was established to transform the local total station coordinates into a Universal Transverse Mercator (UTM), zone 10 North NAD 1983 horizontal map coordinate system. A North American Vertical Datum 1988 (NAVD88) using Geoid Model 2003 (GEOID03) was applied for elevations. Two TOPCON Hiper Lite Plus survey grade GPS receivers were used to establish static control for each plot. The National Geodetic Survey (NGS) Online Position User Service was used for postprocessing control station coordinates.

2.4. GPS Survey

Three different Trimble mapping grade GPS receivers were used for GPS data collection in all eleven plots. These included the GeoXT, GeoXH, and ProXH receivers which all have similar accuracy specifications. We collected GPS data in all plots so that comparisons could be made to total station measurements, the subject of additional research. Based on funding and procurement time lag of the higher accuracy rated ProXH and GeoXH receivers, we chose to begin the project using the GeoXT receiver for data collection in the clearcut and younger even-aged (E412) plots. All but one of the remaining plots was measured using the ProXH, and the final plot data (U8) was collected using the GeoXH based on project time constraints. The GeoXT was configured using the Trimble Hurricane model external antenna while the GeoXH and ProXH were both configured with the Trimble Zephyr external antenna. We used a 15 degree horizon mask, a standard PDOP mask of 6 [29]), and a default signal-to-noise ratio (SNR) value of 39 dB Hz [30].

Similar to the total station survey, each tree, shrub, and tree sweep (where applicable) was measured using a GPS. The GPS receiver and antenna were attached to a pole with the antenna mounted 2.2 m above ground. Large tree locations were measured using a two meter offset and hand compass to maintain a consistent azimuth. All others were measured at the feature location. A minimum of thirty and usually not more than sixty points were collected per position. GPS receiver files were downloaded and differentially corrected using Trimble Pathfinder Office version 4.10. Each file collected using the GeoXT was differentially corrected using course acquisition (C/A) code processing using multiple base station providers selected through proximity to the plot and an integrity index. The original intent was to collect data using dual frequency carrier phase ranging. However, when differentially correcting the data, no carrier phase data corrections were possible. The closest available base providers were chosen, unless the integrity index was below eighty. We selected 80 because a priori knowledge indicated that integrity index values above 80 were consistently achievable. Each file collected using the ProXH or GeoXH receiver was differentially corrected with automatic carrier and C/A code processing using multiple base station providers. When using the multiple base provider option, Pathfinder Office averages the coordinate data from each base station provider in the group, weighting the closer base provider higher to determine a single position solution.

2.5. LiDAR Collection

LiDAR data were collected on 2 April 2008 under clear, sunny weather conditions by Watershed Sciences based in Corvallis, Oregon. A Leica ALS50 Phase II laser system was used with a ±14° scan angle from nadir and pulse rate designed to achieve a point density of ≥8 points per square meter. To reduce laser shadows and increase laser coverage, each flight line had ≥50% side-lap, which equates to ≥100% overlap throughout the study area. The system is capable of a maximum number of four returns per pulse. The onboard differential GPS unit measured aircraft position twice per second (2 Hz) and the inertial measurement unit (IMU) measured aircraft attitude 200 times per second (200 Hz) [31].

Ground control was conducted simultaneously with the airborne LiDAR survey using a static GPS located over ground stations with known locations at a rate of one point collected per second (1 Hz) with indexed time.

The LiDAR data accuracy was described by the vendor as the mean error and standard deviation of the LiDAR point coordinates compared to RTK surveyed ground point coordinates. The vendor provided laser point density and accuracy (Table 3). Although a 1 meter resolution DEM of the ground surface was provided, no methodology or accuracy statistics were made available by the vendor.

Table 3. Laser point density and accuracy reported by vendor.

	Target	Reported
Average First Return Point Density	≥8 points/m^2	10 points/m^2
Average Ground Point Density		1.12 points/m^2
Vertical Accuracy (1σ)	<0.13 m	0.020 m
Average Relative Accuracy		0.053 m
Absolute Accuracy		0.026 RMSE
Absolute Z Accuracy		0.007 ME, 0.026 SD

2.6. LiDAR Processing

Several different algorithms have been developed to delineate individual tree crowns and measure tree heights. We compared three extraction algorithms (methods) including WS segmentation, TreeVaW, and FUSION. The WS segmentation and TreeVaW methods automatically delineate and measure features determined to be trees from the CHM (Figure 3), whereas FUSION requires manual location and measurement of each tree feature from the LiDAR point cloud and, if needed to aid in extraction, a CHM. We used FUSION to create CHM rasters at spatial resolutions of 0.1, 0.3, and 1 m in order to examine resolution influence on tree determination processes. Additionally, FUSION uses mean and median convolution smoothing filters in creating a CHM. The program preserves the local maxima (peaks) while smoothing the surrounding pixels based on the mean or median value of the pixel values within the filter kernel, forcing the surface to adhere to the tree tops. Besides the value of the local maxima, which maintains the value as the highest point in each tree neighborhood, the values of the surrounding crown are stepwise smoothed [28]. We experimented with both filter approaches and found that the mean filter when compared to the field measured data appeared to have increased errors of omission, thus we used the median filter. Filter options tested were: none, 3 × 3, and 5 × 5. We also applied these filter options in examining WS segmentation and TreeVaW output. After running WS segmentation and TreeVaW iteratively using each CHM resolution, two factors were used to select the model that best matched the field survey data. The first factor was the number of trees and the second was spatial variation. The closest matched sum of trees was selected first, and then the spatial variation of the tree points were observed in a GIS. Spatial variation included two subparts: location and pattern. In many cases the LiDAR generated tree count by plot matched the field survey count, however, when viewing the spatial location of the points in a GIS map, it became obvious that errors of commission occurred, e.g., many points were clustered in a location where only one tree was field measured; or many single trees were located in locations that trees did not exist and were well outside a reasonable distance from a field measured tree, thus creating a spatial pattern that did not match the field measured pattern.

Figure 3. Canopy Height Model (CHM) representing **(a)** CHM-Plot C20 Clearcut and **(b)** CHM-Plot O69 old growth plots. Each CHM image represents 100 m^2.

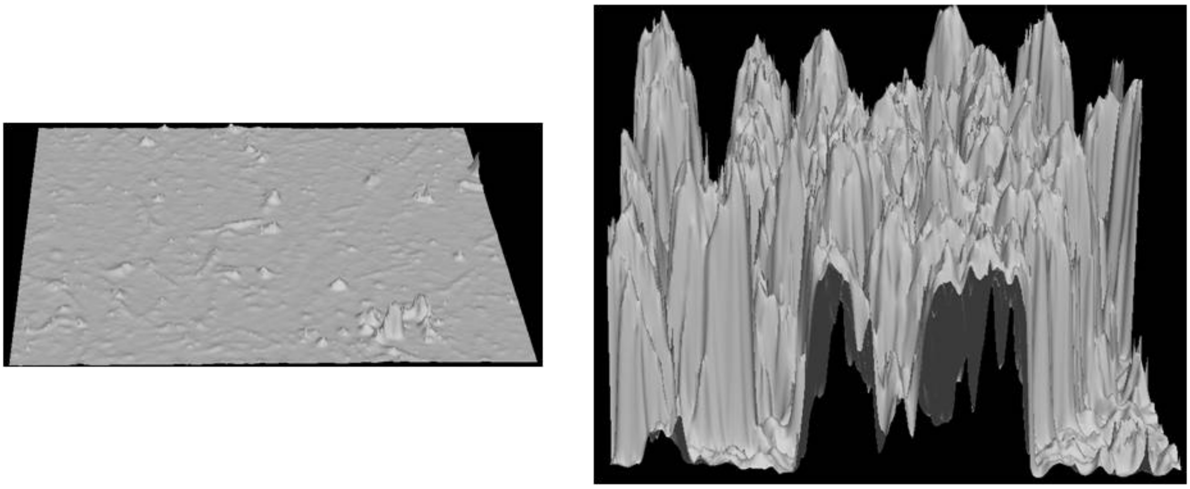

(**a**) (**b**)

ArcGIS software was used to conduct watershed segmentation. Watershed segmentation determines tree locations and heights by inverting the CHM so that when the model is turned upside down the peaks become depressions. When the raster surface is configured as a depression model, watershed segmentation can then be performed to delineate basins (canopy basins). The canopy basin raster model is converted to canopy polygons which delineate a polygon canopy vector file. The model then uses zonal statistics to overlay the canopy basin file on the CHM and assign the highest pixel value per individual tree canopy basin while replacing all other pixels with a no-data value leaving one pixel remaining with a height value per designated canopy. This value becomes the tree height (Z) and tree bole location (X and Y). Two shapefiles are created in the process, one with only a tree X and Y location and another with a tree X and Y location that includes tree height (Z).

We used TreeVaW software version 1.0 [32]. TreeVaW implements the CHM processing software in Interface Definition Language (IDL) to locate and measure trees. TreeVaW uses the CHM in ENVI image format and produces output consisting of tree positions in x and y coordinates, tree heights, and crown radii [32]. The "VaW" in TreeVaW is an acronym for variable window. The program delineates trees by deriving an appropriate size circular search window to find tree tops from the CHM based on the relationship between the height of trees and their crown size. As found in nature, the taller the tree, the larger the crown size [12]. The program is designed for conifer forest applications and uses a search window based on a default regression relationship of crown diameter as a function of height developed in the southeastern United States, thus the crown diameter relationship was edited using the field collected data for this project. The program's default regression formula is $CW = 2.51503 + 0.012000\ H^2$ where CW is crown width and H is height. Initial attempts at TreeVaW tree delineation met with poor results in clearcut plots when the regression equation from all field collected trees was used, thus a separate equation was used for the clearcut plots based only on the field database of clearcut plot conifer species. Three attempts were made to determine which regression equation to use for delineating trees in clearcut plots and are further discussed in the results section. For all other plots, the field collected database of all trees except snags having no crown was used for the regression. Dead trees with discernable crowns were included. The input of minimum and maximum crown width and maximum expected tree height parameters are also required before running TreeVaW. We input these values based on our field data.

We applied FUSION software version 2.70 [33] for tree delineation. The FUSION software consists of two main programs, FUSION and the LiDAR data viewer (LDV). Many component command line programs also come with the FUSION package for preparing and processing raw LiDAR data for analysis in FUSION and LDV. Once pre-processing steps are completed and the LiDAR data are prepared for plot level analysis, trees are manually selected and measured in LDV using the LiDAR point cloud (Figure 4(a)) and measurement marker (Figure 4(b)). Although canopy base height was not measured by field crews in our study, of the three LiDAR software programs used in the study, FUSION is the only one capable of this measurement. In the FUSION generated plots, we measured heights of the upper portion of the point cloud, which in most cases is likely the top of the crown and not the apex of the tree, and measured the lowest discernible portion of the point cloud coincident with what appeared to be the lowest whorl of branches. This was only possible in larger trees in primary canopy where sufficient returns were available to identify the minimum and maximum crown heights. Crown diameter was measured using the measurement marker in either a circular form for a generally round-shaped crown, or elliptically where the crown was more oval-shaped from an orthogonal perspective. Spatial x and y location was measured based on where the analyst determines the apex and center of the tree to be located. Each set of measurements is added to a Comma Separated Value (CSV) file database of individual trees.

Once the LiDAR was prepared for each software program used in this study, there were significant differences in time required to delineate trees. Both TreeVaW and watershed segmentation were automated tree delineation programs that processed each hectare sized plot in this study rapidly within seconds. FUSION on the other hand requires the operator to manually measure and save each tree. This process is relatively quick (30–60 seconds per tree) for large trees in the primary canopy, but becomes progressively more difficult to differentiate smaller trees in the sub-canopy. Based on the time required to delineate individual trees using FUSION, and that this project involved thousands of trees, we limited tree delineation using FUSION to six plots (C110, E200, O16, O69, U8, U13). The advantage to using TreeVaW and watershed segmentation is the speed of processing. The disadvantage to these two programs is that they are limited by the CHM, which inherently due to interpolation loses tree information below the upper canopy. The advantage of FUSION is that it uses the LiDAR point cloud, where all points are available to the user.

Field measured tree X and Y locations and tree heights were compared to those determined by each LiDAR extraction method. For this study, the main purpose of comparing the accuracy of each tree's spatial location was to establish confidence that tree height comparisons between ground and LiDAR were based on the same tree. The only confirmation of this was similar spatial location and height. The most accurate method used for determining tree spatial location in this study was by total station survey instrument.

Figure 4. (a) FUSION LiDAR Data Viewer (LDV) measurement window displaying tree height measurement capability. Tree X and Y location, height, crown width, crown base height, and elevation at tree base may be measured and saved to file; **(b)** FUSION measurement marker surrounding a single LiDAR tree.

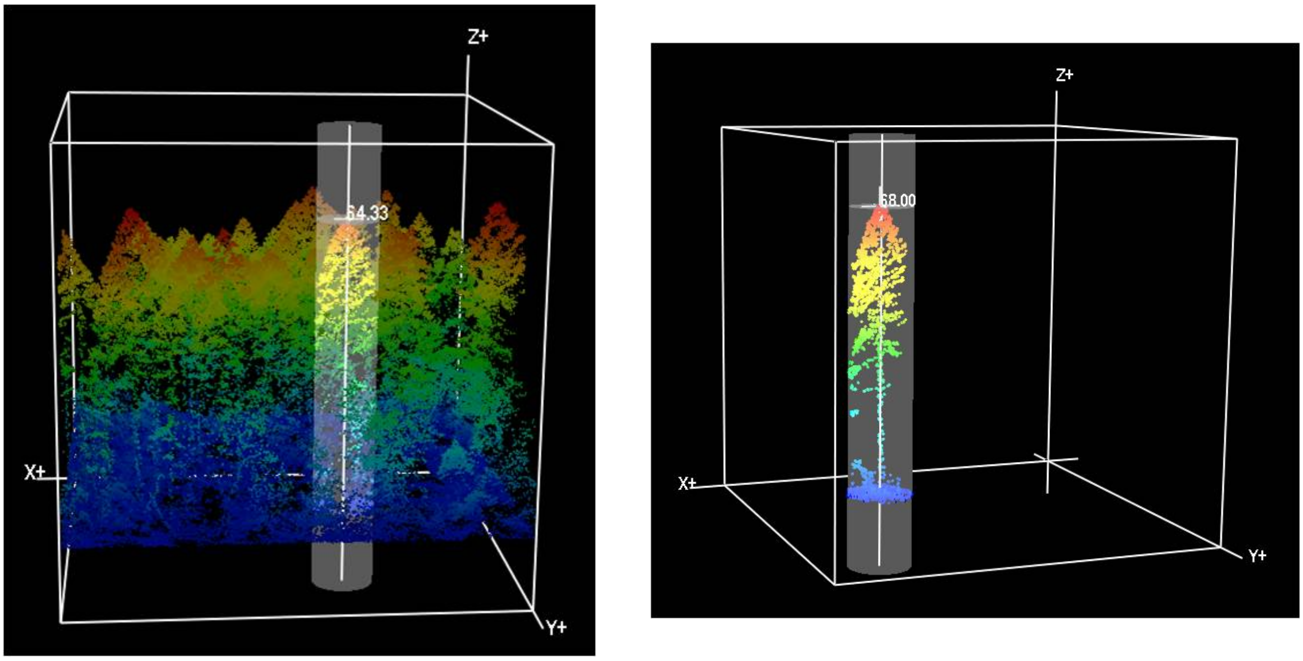

(a) **(b)**

2.7. Geographic Information System (GIS) Processing

Tree and shrub locations were measured by total station on five of the eleven plots as discussed above. Height and species was nominally noted, *i.e.*, tree heights were noted as small, average, large, or extra large for the respective plot. Species was noted as conifer or broadleaf. GPS measurements were made in all 11 plots. In addition to absolute spatial location, tree height, crown radius, and species were determined and recorded. In the total station surveyed plots, the specific tree data collected in the GPS survey was used to match total station surveyed trees such that the most accurate horizontal coordinates were combined with specific species and height measurements. Total station feature points were matched to those determined by GPS using ArcGIS software. Each tree feature was matched manually, based on proximity, height (absolute to nominal), and species (specific to nominal) and assigned the same unique identification number. Trees were only matched if relative confidence existed that the two represented the same tree. Where there was doubt, features were not matched. The least amount of confidence in matching occurred in the even-aged plot (E200), where most of the trees were a similar height and species (Douglas-fir). Proximity was the only matching metric, thus some bias may exist in horizontal error between tree locations determined by GPS and total station.

2.8. Biomass

Total above ground biomass (TAGB) was calculated using allometric equations from the biomass computation package BIOPAK [34] (Table 4). Because we measured only height and crown diameters for shrubs, and did not measure stem or basal diameters we chose to use percent crown cover for shrub

TAGB estimates. We used GIS software to calculate crown cover by creating a polygon layer using the field measured crown diameter measurements for all shrubs in the plot, clipping the shrub crown polygon layer using the plot perimeter data, and then calculating percent crown cover for the 1 ha plot. The majority of the shrubs in the study area were California hazel (*Corylus cornuta*), thus we used this species to calculate a general shrub TAGB estimate on a by-plot basis. The closest allometric equations using crown cover we could find for our study area were based on destructive sampling of California hazel collected in riparian zones and meadows in the Sierra Nevada, California. The equation used was BAT = (5.01 × COV) × m^2. BAT is TAGB including foliage, COV is the cover percentage, and m^2 is the plot dimension in square meters [34]. Crown (canopy) cover is the proportion of vertically projected tree or shrub crown (above ground vegetation) that covers the forest floor measured as the presence or absence of canopy vertically above sample points across an area of forest. The height of the tree or shrub has no impact on this measurement as it is the vertical projection of the crown that is measured. Crown cover may be used to predict volume by species because crown area to trunk (stem) basal area has a near linear relationship (biomass) [35]. All tree TAGB estimates were based on allometric equations related to DBH or DBA, with some equations including height. For trees smaller than 0.13 m DBH, the DBA equations were used. Where weights were calculated in cm^3, weights were converted to kg. All LiDAR TAGB estimates were based on Douglas-fir TAGB estimates. Two Douglas-fir equations were used, one for trees ≥0.13 m DBH and trees <0.13 m (Table 4) based on BIOPAK values [34]. BIOPAK provides a Coast Range region equation for small trees whose stem diameter is measured at the base and another based on DBH of larger trees). We used a cutoff of 0.13 m DBH for large and small trees. If a tree was smaller than 0.13 m DBH, then the stem diameter was measured at ground level (DBA). LiDAR DBH estimates were based on regression analysis from trees measured in this study.

3. Results

3.1. LiDAR Model Selection

Stem count spatial variation were used to compare LiDAR model results to field measurements (Table 5). Each method resulted in various errors of omission and commission. For WS segmentation and TreeVaW, we experimented with different resolution CHMs interpolated from the original LiDAR point clouds. When using a CHM, any vegetation below the dominant/co-dominant canopy is likely to fall below the CHM surface, thus we experimented with higher resolutions to determine if smaller trees could be discernible within the LiDAR data. In some cases clustering was observed where errors of commission occurred. One example of this was many tree points clustered around only one field-surveyed tree. In some cases this was due to multiple hits on a single broadleaf tree and in others, false tree tops on a conifer tree. Errors of commission were also observed where a tree was delineated in a location where no field surveyed tree existed. This was primarily due to higher resolution CHM interpolation causing errors of commission. The 0.1 m resolution was decisively in error compared to the other, coarser resolutions. The best matching LiDAR designated results also had instances of clustered points around a single field surveyed vegetation point, which in most instances appeared to be multiple hits on a broadleaf tree such as bigleaf maple.

Table 4. Equations used to determine plot biomass from biomass computation package BIOPAK [34].

Species	Bio Component Description	Region *	Biomass Equation
Abies amabilis (Pacific silver fir)	BAT = Total aboveground biomass	G	BAT = 12,800 + 0.1836 × DBH^2 × HT
Abies grandis (grand fir)	BAT = BAT without dead branches	G	BAT = 30.2 + 146.9 × DBH^2 × HT
Acer circinatum (vine maple)	BFT = Total foliage biomass	W	ln(BFT) = 1.8820 + 1.9754 × ln(DBA)
Acer circinatum (vine maple)	BST = Total stem biomass	W	ln(BST) = 3.1591 + 2.5335 × ln(DBA)
Acer macrophyllum (bigleaf maple)	VAE = Volume (cm^3) above grd.	C	ln(VAE) = 1.623161 + 2.22462 × ln(DBH) + 0.57561 × ln(HT)
Arbutus menziesii (Pacific madrone)	BAT = Total aboveground biomass	C	BAT = −1,080 + 918.92 × DBA^2
Berberis repens (Oregon grape)	BAT = Total aboveground biomass	G	ln(BAT) = 2.976 + 2.092 × ln(DBA)
Cornus nuttallii (Pacific dogwood)	BFT = Total foliage biomass	W	ln(BFT) = 2.7920 + 1.8685 × ln(DBA)
Cornus nuttallii (Pacific dogwood)	BBL = Live branch biomass	W	ln(BBL) = 2.2606 + 2.8737 × ln(DBA)
Cornus nuttallii (Pacific dogwood)	BST = Total stem biomass	W	ln(BST) = 3.2943 + 2.0625 × ln(DBA)
Corylus cornuta californica (Cal. hazel)	Cover	S	BAT = 5.01 × COV
Holodiscus discolor (oceanspray)	BAT = Total aboveground biomass	R	ln(BAT) = 3.769 + 3.033 × ln(DBA)
Pinus ponderosa (ponderosa pine)	BAT = Total aboveground biomass	G	BAT = 1,160 + 0.1870 × (DBH)2 × HT
Populus trichocarpa (black cottonwood)	BAT = BAT without dead branches	G	BAT = 7,400 + 0.1564 × DBH^2 × HT
Prunus emarginata (bitter cherry)	BAT = Total aboveground biomass	E	ln(BAT) = −9.27455 + 2.8934 × ln(LEN+WID)
Pseudotsuga menziesii (Douglas-fir)	BAT (Large trees) = Biomass aboveground (w/o dead branches)	C	ln(BAT) = 4.7824 + 2.2985 × ln(DBH)
Pseudotsuga menziesii (Douglas-fir)	BAT (small trees) = Geometric mean stump dia.above grd biomass.	C	ln(BAT) = 4.59314 + 2.03553 × ln(DBA)
Quercus garryana (Oregon white oak)	VAE = Volume (cm^3), above ground. live+dead wood plus bark	G	ln(VAE) = 0.793195 + 2.14321 × ln(DBH) + 0.7422 × ln(HT)
Thuja plicata (western redcedar)	BAT = Total aboveground biomass	G	BAT = 40,400 + 0.0969 × DBH^2 × HT
Tsuga heterophylla (western hemlock)	BAT = Total aboveground biomass	G	BAT = 29,800 + 0.1558 × DBH^2 × HT
Umbellularia californica (Cal. laurel)	VAE = Volume (cm^3), above grd. live + dead wood plus bark	C	ln(VAE) = 0.2643834 + 1.94553 × ln(DBH) + 0.88389 × ln(HT)

* Region abbreviations: G: General, W: Western Cascades, C: Coast Range, E: Eastern Cascades, R: Rocky Mountains.

Table 5. Delineated stem counts resulting from watershed segmentation using various CHM resolutions compared to field measured vegetation. Checked numbers indicate the resolution and filter method that best matched field count numbers.

Plot	0.1 m, 5 × 5 Filter	0.3 m, 3 × 3 Filter	0.3 m, 5 × 5 Filter	1 m, No Filter	Field Count Tree/Shrub	Field Count Total	LiDAR/Field Count (%) all/tree only*
C20	6,780	948	595	825✓	691/8	699	118/119
C27	1,249	366	250	647✓	565/15	580	111/115
C61	3,969	684	411	632✓	534/0	534	118/118
C110	3,535	381	247	619✓	575/118	693	89/108
E200	6,848	1,067✓	776	476	946/56	1,002	107/113
E412	12,268	1,540	957✓	546	929/57	986	97/103
O16	14,728	2,049	999	210✓	363/140	503	42/58
O69	14,769	1,736	974	222✓	257/45	302	73/86
U8	19,994	1,727	991	191✓	367/153	520	37/52
U13	18,312	1,623	688	311✓	498/47	545	57/62
U56	17,331	1,523	824✓	256	1,255/72	1,327	62/66
Total		1,067	1,781	3,657			
Grand Total		6,505 (from ✓ selected values)			6,980/711		85/93

* Percent of best matching LiDAR count to field count total and trees only.

A one meter resolution CHM interpolated without a convolution filter resulted in watershed segmentation tree designations that appeared to best match field measured trees (Table 5). Three exceptions to this were in the even-aged plots and one uneven-aged plot. In plot E412 the 0.3 resolution CHM using 3 × 3 and 5 × 5 filters displayed the spatial pattern obviously created by planting in rows, and the 5 × 5 filter best matched the number of stems to field measured. The GPS field collected data did not reflect this pattern based on random spatial error caused by the GPS. TreeVaW did not display this pattern either except when using the 0.3 m resolution canopy height model with a 3 × 3 filter.

Several iterations were run in the clearcut plots to find the best match of TreeVaW delineated trees to field measured trees (Table 6). The two decision factors used to determine the best match for TreeVaW were numbers of trees and spatial relationship as discussed in methods. The first iteration utilized the crown to tree height relationship from all field measured trees (minus snags with no crown): CW = 0.0028 + 1.1207 × (H), where CW = crown width and H = tree height (R^2 = 0.74). TreeVaW also requires inputs of expected maximum height and crown widths. We used expected values for the entire project which were based on maximum ground measured heights and crown widths from all plots combined. The second iteration used the same crown to tree height relationship but the required inputs of maximum tree height and crown width were limited to sizes expected only in the clearcut plots, which were determined from our field sampled database of all clearcut plot trees. The third iteration used the crown to tree height relationship found only in clearcut plot conifer trees, CW = 0.09550 + 0.5173 × (H) (R^2 = 0.77), and the required input of tree height and crown width remained limited to sizes expected in clearcut only plots, also determined from our database of field sampled clearcut conifer trees. All other plots besides clearcut plots used the crown to tree height relationship of CW = 0.0028 + 1.1207 × (H). Individual tree measurements are saved in a text file including height, spatial location, and crown radius. Crown radius is used for generation of circular crown buffers in GIS, thus converting the radius into a diameter. Each TreeVaW text file was then converted to an ESRI shapefile for GIS analysis.

Table 6. TreeVaW LiDAR stem counts compared to GPS and total station field counts. Checked numbers indicate the resolution and filter method that best matched field measured trees based on count and spatial relationship.

Plot	CHM Resolution and Filter Size				GPS Field Count Tree/Shrub	Total Station Count Tree/Shrub	Difference (%)/tree n *
	0.1 m, 5 × 5 Filter	0.3 m, 3 × 3 Filter	0.3 m, 5 × 5 Filter	1 m, No Filter			
C20	98/385/385	102/132/70	✓96/135/52	98/172/98	×691/8	N/A	14/14
C27	16/51/51	95/54/53	65/51/39	58/✓115/58	×565/15	N/A	19/20
C61	776/316/316	120/108/78	193/112/57	✓82/111/62	×534/0	N/A	15/15
C110	281/540/540	165/81/105	✓104/80/58	101/182/101	×575/118	N/A	15/18
E200	973	664	✓704	616	×946/56	910/78	70/74
E412	2,507	✓1,049	475	664	×929/57	N/A	106/113
O16	822	197	✓218	114	×363/140	355/173	43/60
O69	1,129	276	✓197	125	238/-	×257/45	65/77
U8	1,243	✓123	118	88	192/-	×367/153	24/34
U13	1,987	457	✓285	211	×498/47	385/48	52/57
U56	✓1,117	276	187	167	×1,255/72	N/A	84/89
Total	1,117	1,172	1,604	197			
Grand Total		4,090 (from ✓ selected values)			** 6,980/711		53/59

Clear cut iterations are listed in order from left to right third, second, and first iteration. * Percent of best matching LiDAR count to field count total and trees only. Field counts used were based on the GPS inventory, with the exception of Plots O69 and U8 where GPS excluded shrubs. ** Shaded counts with an × indicate values used to calculate totals.

GIS point files were generated from field measured data and each of the three tree extraction software programs used in this study (Figure 5). Visual inspection of tree patterns suggest that all methods compare relatively well to the field measured points for Plot E200 as little canopy height differentiation existed. In plots O16 and U13, strictly looking at numbers, the watershed segmentation achieves the greatest number of trees, followed by TreeVaW and FUSION (Table 7). The most obvious pattern is displayed in plot E200. Tree planting pattern is observed using all methods, the least obvious of which is the field measured data likely due to the random horizontal error associated with mapping grade GPS.

3.2. LiDAR Count Comparison

Comparing each method of LiDAR tree detection shows a great deal of variation in the number of trees detected in each plot with manual detection trees in FUSION consistently delineating fewer (Table 7), noting that FUSION was only used on six plots. Based only on field measured tree counts, tree delineation was best performed by watershed segmentation followed by TreeVaW and FUSION with overall percentages equaling 93%, 59%, and 44% respectively. Watershed segmentation appeared to perform noticeably better on the clearcut and even aged with the exception of plot E412 where TreeVaW had a similar percentage (Table 7). All methods did considerably poorer in uneven aged and old growth treatments due primarily to missing understory trees.

Figure 5. LiDAR tree extraction method comparison for plots representing even aged (E200), old growth (O16), and uneven aged (U13) conditions. The figure rows (ordinate) contain images of the plotted tree/vegetation stem locations by method and the columns (abscissa) are the corresponding plots. Field measured points are displayed with trees (solid dots), shrubs (hollow dots), and with trees only.

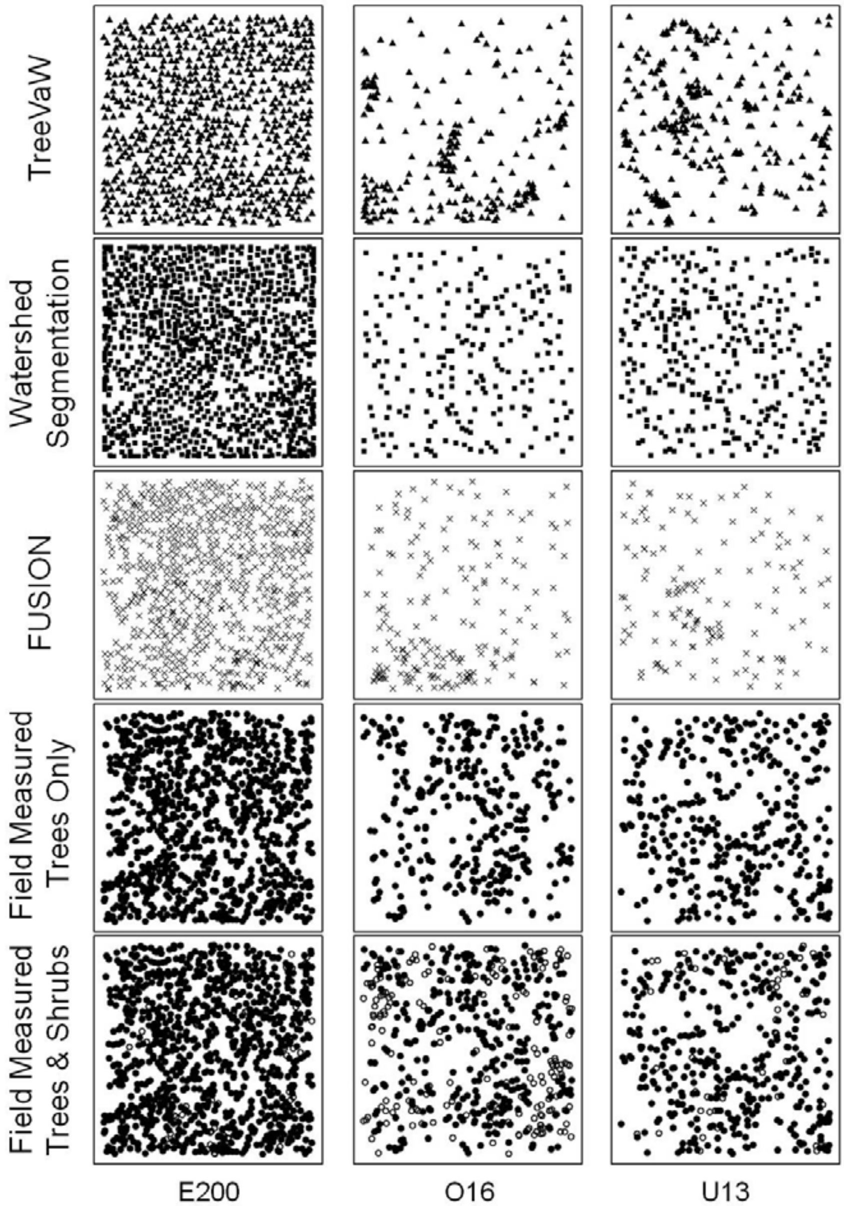

Each program was relatively consistent when manually matching trees to field measured tree points in a GIS (Table 8). FUSION again demonstrated the fewest matches, followed by TreeVaW and watershed segmentation. FUSION was within 16% (969) and TreeVaW 14% (994) of the count achieved by watershed segmentation (1,151). In this portion of the study, only trees that were within a reasonable distance (based on height) and similar height were compared. Taller trees were subjectively given greater manual search windows based on having larger crowns that could potentially be struck by LiDAR pulses.

Table 7. Tree feature count by LiDAR extraction method compared to field count by total station and GPS.

Plot	WS Segment.	TreeVaW	Fusion Count	GPS Tree/Shrub	GPS Field Count Total	Total Station Count Tree/Shrub
C20	825	96	N/A*	691/8	699	N/A*
C27	647	115	N/A	565/15	580	N/A
C61	632	82	N/A	534/0	534	N/A
C110	619	104	184	575/118	693	N/A
E200	1067	704	652	946/56	1,002	910/78
E412	957	1049	N/A	929/57	986	N/A
O16	210	218	181	363/140	503	355/173
O69	222	197	86	238/-	238	257/45
U8	191	123	88	192/-	192	367/153
U13	311	285	135	498/47	545	385/47
U56	824	1,117	N/A	1,255/72	1,327	N/A
Total	6,505	4,090	1,326	Field Count 6,980/711		
% of Fld Count (all/trees).	85/93	53/59	37/44			

* N/A indicates that FUSION or total station summaries were not performed on this plot.

3.3. LiDAR Height Comparison

We compared field measured and LiDAR derived tree heights using three comparisons. The first comparison was conducted on select plots by matching and pairing individual features as explained in methods. Height errors between the three methods of extracting LiDAR features compared to ground measurements were initially calculated by tree. Average height errors, standard deviations (SD), and root mean square errors (RMSE) were then calculated for five plots (plots E200, O16, O69, U8, and U13) where field total station measurements were made (Table 8). Additionally, the same height comparison was performed for one clearcut plot (plot C110) where only field GPS measurements were made. This second height comparison is differentiated from the other by three primary factors: field spatial location measurement, field height measurement, and silvicultural treatment. The spatial locations were measured by GPS, tree heights were measured using a height pole, and the silvicultural treatment was a clearcut consisting of seedlings. The difference in the clearcut is important because the trees were small, but no overstory existed to prevent the LiDAR pulses from striking the tree. Since overstory was not a factor, then the primary factor impacting whether a tree was detected is LiDAR pulse density. Another factor is that the point matching was completed manually in FUSION. We found it difficult to identify small trees in FUSION and believed this to be primarily due to overstory obscuration. We wanted to determine if small trees could be detected in FUSION when no overstory obscuration existed. Because of these differences, we chose to display this comparison separately. A third comparison evaluated plot averages for all study plots.

Table 8. LiDAR tree extraction method comparing spatial location and average and absolute tree height* error (m) to field measurements.

Plot	Method	Statistic	X_{TS} − X_{LiDAR}	Y_{TS} − Y_{LiDAR}	Horizontal Difference	Field Height − LiDAR Height	Trees
E200	**FUSION**	Avg. (Abs.)	0.29	0.03	1.66	0.41 (0.86)	589
		SD (RMSE)	1.50	1.29	1.10 (1.99)	1.27 (1.33)	
	TreeVaW	Avg. (Abs.)	0.14	0.02	1.70	0.50 (0.91)	620
		SD (RMSE)	1.50	1.34	1.08 (2.02)	1.25 (1.35)	
	WS Seg.	Avg. (Abs.)	−0.35	−0.18	1.73	0.52 (0.96)	691
		SD (RMSE)	1.49	1.32	1.06 (2.03)	1.28 (1.38)	
O16	**FUSION**	Avg. (Abs.)	−0.48	−0.50	2.95	−0.22 (1.33)	119
		SD (RMSE)	2.73	2.45	2.28 (3.72)	2.19 (2.19)	
	TreeVaW	Avg. (Abs.)	−0.89	−0.14	3.59	0.15 (1.79)	86
		SD (RMSE)	3.51	2.29	2.32 (4.27)	2.62 (2.61)	
	WS Seg.	Avg. (Abs.)	−0.63	−0.33	3.52	0.17 (1.74)	104
		SD (RMSE)	3.03	2.97	2.45 (4.28)	2.49 (2.49)	
O69	**FUSION**	Avg. (Abs.)	−0.23	−1.34	2.72	−2.72 (3.79)	70
		SD (RMSE)	2.37	1.97	1.96 (3.35)	4.22 (4.99)	
	TreeVaW	Avg. (Abs.)	−0.17	−0.53	3.36	−1.75 (3.50)	72
		SD (RMSE)	3.92	2.38	3.15 (4.59)	4.52 (4.82)	
	WS Seg.	Avg. (Abs.)	−0.34	−0.73	2.97	−1.97 (3.73)	71
		SD (RMSE)	2.66	2.34	2.06 (3.61)	4.69 (5.05)	
U8	**FUSION**	Avg. (Abs.)	0.36	0.32	1.66	−1.29 (3.44)	83
		SD (RMSE)	1.16	1.65	1.24 (2.06)	4.90 (5.04)	
	TreeVaW	Avg. (Abs.)	0.11	0.01	1.78	−0.02 (2.79)	74
		SD (RMSE)	1.41	1.89	1.53 (2.34)	4.31 (4.29)	
	WS Seg.	Avg. (Abs.)	0.18	0.34	2.19	−0.44 (3.43)	108
		SD (RMSE)	2.19	1.94	1.97 (2.94)	5.02 (5.02)	
U13	**FUSION**	Avg. (Abs.)	−0.12	−0.22	3.04	−0.06 (1.14)	108
		SD (RMSE)	2.86	2.69	2.48 (3.91)	1.52 (1.51)	
	TreeVaW	Avg. (Abs.)	0.07	−0.12	3.14	0.25 (1.22)	142
		SD (RMSE)	3.03	2.42	2.27 (3.87)	2.16 (2.16)	
	WS Seg.	Avg. (Abs.)	0.00	−0.23	3.67	0.34 (1.13)	177
		SD (RMSE)	3.52	3.10	2.91 (4.68)	1.59 (1.62)	
Total	**FUSION**	Avg. (Abs.)	0.12	−0.14	2.05	−0.09 (1.38)	969
		SD (RMSE)	1.94	1.79	1.67 (2.64)	2.43 (2.43)	
	TreeVaW	Avg. (Abs.)	0.02	−0.06	2.19	0.28 (1.23)	994
		SD (RMSE)	2.24	1.76	1.83 (2.85)	1.86 (1.88)	
	WS Seg.	Avg. (Abs.)	−0.27	−0.19	2.31	0.22 (1.46)	1,151
		SD (RMSE)	2.23	2.01	1.94 (3.02)	2.45 (2.46)	

* Field measured tree spatial location and height were determined by total station and laser rangefinder respectively.

In the total station to LiDAR comparisons, three plots (E200, O16, and U13) had mean height errors no greater than 0.52 m (SD 1.28 m). Among these three plots, the largest average mean height error was in plot E200 with the watershed segmentation method and the lowest was in plot U13 at −0.06 m (SD 1.52 m) (Table 8). The overall greatest amount of height error occurred in plot O69 (−2.72 m (SD 4.22)) with FUSION. Plot 069 also had the most error when comparing LiDAR approaches across plots.

Height errors in O69 may have been impacted by the plot's severe sloping terrain. When comparing the height measurement results using a paired t-test, plots E200 and O69 were significantly different for all LiDAR techniques except one ($p < 0.01$), thus indicating that there is a high probability that mean tree heights measured by LiDAR compared to those measured by laser range finder are generally not the same (Table 9). The lone exception occurred in plot E200 for the watershed segmentation results ($p = 0.19$). Statistically significant differences also occurred with FUSION in plots O16 and U8. The significant differences that were determined in plot E200 are noteworthy because this plot is generally a monoculture of Douglas-fir planted at the same time and having a similar mean height. For these reasons, plot E200 is the plot most expected to have similar results when comparing LiDAR results to field measurements.

Table 9. Statistical comparison of paired LiDAR-derived tree heights to laser range finder (LRF) tree heights.

Plot	Avg LRF Height *	Avg LiDAR Height	df	t-stat	*p*-value
E200					
FUSION	14.09	13.69	588	4.59	<0.01
TreeVaW	13.85	13.35	619	5.94	<0.01
WS Seg.	13.75	13.24	690	1.30	0.19
O16					
FUSION	34.98	35.19	118	−2.34	0.02
TreeVaW	33.66	33.51	85	1.36	0.18
WS Seg.	37.06	36.89	103	−0.76	0.45
O69					
FUSION	41.53	44.25	69	−5.39	<0.01
TreeVaW	35.04	36.79	71	−3.28	<0.01
WS Seg.	39.45	41.43	70	−3.54	<0.01
U8					
FUSION	44.39	45.68	82	−2.40	0.02
TreeVaW	36.90	36.92	73	−0.04	0.97
WS Seg.	38.37	38.81	107	−0.91	0.36
U13					
FUSION	18.48	18.54	107	−0.13	0.90
TreeVaW	14.15	13.90	141	1.15	0.25
WS Seg.	13.28	12.93	176	0.16	0.88

* Field measured tree spatial location and height were determined by mapping grade GPS and height pole respectively.

For the one clearcut plot (C110) where height comparisons were made by tree matching, height measurements were compared between field horizontal measurements determined by mapping grade GPS and height measurements determined mostly by height pole to the same measurements determined by the three LiDAR extraction methods (Table 10). In this plot it appeared that shrubs were detected as no canopy existed to prevent LiDAR pulses from reaching shrubs. In all plots except for the clearcut plots it appeared shrubs were not detected due to LiDAR pulse obstruction by canopy. This observation is based on manual observations of point clouds in FUSION, and features delineated in watershed segmentation and TreeVaW that did not correspond to field measured shrub locations, and LiDAR heights that indicated trees rather than shrubs. The least amount of error occurred when comparing TreeVaW trees to field measured, however only 17 trees could be matched. The greatest amount of error was 1.27 m (SD 0.51 m) comparing shrubs detected by watershed segmentation to field measurements. The second least amount of error was 1.17 m with watershed segmentation and FUSION in detecting shrubs and trees, respectively.

Table 10. LiDAR tree extraction method comparing spatial location and height (m) of trees and shrubs to field measurement in one clearcut plot.

Plot	Statistic	X_{TS} minus X_{LiDAR}	Y_{TS} minus Y_{LiDAR}	Horizontal Difference	Field Height minus LiDAR Height *	n Paired
	C110 Trees					Trees
FUSION	Avg. (Abs.)	−0.93	0.42	1.42	0.56 (1.08)	83
	SD (RMSE)	0.82	0.81	0.59 (1.53)	1.07 (1.36)	
TreeVaW	Avg. (Abs.)	−0.71	1.46	2.63	0.28 (1.30)	16
	SD (RMSE)	1.92	2.33	2.15 (3.35)	1.69 (1.56)	
WS Seg.	Avg. (Abs.)	−1.07	0.42	1.59	1.17 (1.23)	339
	SD (RMSE)	0.85	2.14	2.02 (2.57)	0.68 (1.37)	
	C110 Shrubs					Shrubs
FUSION	Avg. (Abs.)	−1.03	0.67	1.30	1.17 (1.17)	44
	SD (RMSE)	0.42	0.40	0.38 (1.36)	0.48 (1.26)	
TreeVaW	Avg. (Abs.)	−0.98	0.60	1.23	0.97 (0.97)	4
	SD (RMSE)	0.49	0.37	0.32 (1.26)	0.59 (1.10)	
WS Seg.	Avg. (Abs.)	−1.13	0.53	1.37	1.27 (1.27)	57
	SD (RMSE)	0.62	0.49	0.56 (1.48)	0.51 (1.37)	

* Average (avg.) and absolute (abs.) height differences provided.

Statistically significant height errors ($p < 0.01$) (Table 11) were observed with all methods in the clearcut plot except with TreeVaW, but only sixteen and four features were compared in trees and shrubs respectively and with this method.

Table 11. Statistical comparison of LiDAR-derived tree heights (h) to height pole measured (HP) tree heights in one clearcut plot.

Plot	µ (HP h) − (LiDAR h) (m)	(HP h) − (LiDAR h) 95% CI (m)	df	t-stat	*p*-value
C110 Trees					
FUSION	0.56	0.24 − 1.46	82	2.93	<0.01
TreeVaW	0.28	−0.66 − 1.21	15	−2.00	0.54
WS Seg.	1.17	1.04 − 1.33	338	22.45	<0.01
C110 Shrubs					
FUSION	1.17	1.01 − 1.30	43	16.31	<0.01
TreeVaW	0.97	−0.16 − 2.10	3	2.33	0.08
WS Seg.	1.27	0.94 − 1.59	56	18.72	<0.01

Comparing all field laser range finder (LRF) height measurements to the three methods of LiDAR height measurements in each plot using a Welch modified two-sample t-test resulted in significant differences (p < 0.01) in all comparisons but four (Table 12). Results were inconclusive with TreeVaW in plot O16 (p = 0.68) and O69 (p = 0.83); and with watershed segmentation in plot C61 (p = 0.95) and E200 (p = 0.46).

Table 12. Statistical comparison of mean LiDAR tree heights (h) to field measured (FM) tree heights as measured by a laser range finder.

Plot	Method	Average Height (m)	(μ FM h) − (μ LiDAR h) 95% CI (m)	df	t-stat	*p*-value
C20	Field Measured	1.06				
	FUSION		NOT MEASURED			
	TreeVaW	1.20	−1.46 − (−1.11)	451	−14.54	<0.01
	WS Seg.	0.87	0.08 − 0.31	1067	3.34	<0.01
C27	Field Measured	1.04				
	FUSION		NOT MEASURED			
	TreeVaW	2.50	−1.75 − (−1.18)	125	−10.05	<0.01
	WS Seg.	0.53	0.16 − 0.33	1,207	5.66	<0.01
C61	Field Measured	1.70				
	FUSION		NOT MEASURED			
	TreeVaW	15.03	−15.57 − (−11.09)	189	−11.75	<0.01
	WS Seg.	1.68	−0.49 − 0.53	1,091	0.06	0.95
C110	Field Measured	1.87				
	FUSION	2.06	−0.39 − 0.00	256	−1.93	0.05
	TreeVaW	3.16	−1.55 − (−1.03)	206	−9.79	<0.01
	WS Seg.	0.97	0.78 − 1.01	1,189	15.67	<0.01
E200	Field Measured	12.52				
	FUSION	13.67	−1.37 − (−0.94)	1,482	−10.67	<0.01
	TreeVaW	13.02	−0.74 − (−0.27)	1,724	−4.23	<0.01
	WS Seg.	12.43	−0.14 − 0.31	1,807	0.74	0.46
E412	Field Measured	6.56				
	FUSION		NOT MEASURED			
	TreeVaW	4.69	1.74 − 2.01	1,855	27.80	<0.01
	WS Seg.	4.45	1.95 − 2.28	1,819	25.60	<0.01
O16	Field Measured	18.86				
	FUSION	31.16	−15.22 − (−9.39)	334	−8.31	<0.01
	TreeVaW	19.46	−3.51 − 2.30	390	−0.41	0.68
	WS Seg.	35.15	−19.14 − (−13.44)	384	−11.23	<0.01
O69	Field Measured	20.22				
	FUSION	43.94	−28.15 − (−19.29)	147	−10.58	<0.01
	TreeVaW	19.81	−3.28 − 4.10	387	0.22	0.83
	WS Seg.	31.49	−14.86 − (−7.68)	436	−6.17	<0.01
U8	Field Measured	18.00				
	FUSION	45.65	−29.80 − (−25.51)	417	−25.37	<0.01
	TreeVaW	25.97	−11.94 − (−4.01)	188	−3.97	<0.01
	WS Seg.	35.56	−20.12 − (−15.00)	490	−13.47	<0.01
U13	Field Measured	6.67				
	FUSION	16.66	−12.86 − (−7.13)	177	−6.88	<0.01
	TreeVaW	10.53	−5.64 − (−2.10)	465	−4.29	<0.01
	WS Seg.	16.18	−11.54 − (−7.48)	456	−9.20	<0.01

Table 12. *Cont.*

U56	Field Measured	6.66				
	FUSION		NOT MEASURED			
	TreeVaW	15.18	−10.49 − (−6.57)	329	−8.55	<0.01
	WS Seg.	26.69	−21.02 − (−19.05)	1,615	−39.79	<0.01

3.4. LiDAR Horizontal Comparison

The LiDAR detected and delineated tree horizontal location compared to known locations of field measured trees were similar in each method (Table 8). The least horizontal difference between LiDAR measured trees occurred with FUSION software in all plots. The overall mean horizontal difference between field measured trees and LiDAR-measured trees by FUSION, TreeVaW, and watershed segmentation were 2.05, 2.19, and 2.31 m respectively. The horizontal difference by method can be explained by the precision of the measurement method. FUSION utilizes the point cloud compared to other methods, which use the raster-based CHM. Measurement of the spatial location of a tree in FUSION is based on identifying the single highest discrete point. Error may be introduced by the operator who may not align the measurement marker precisely with the highest point. Methods that rely on a CHM also rely on the highest point however this point is represented by a raster cell (pixel), with a precision that is limited by the resolution of the cell and a coordinate location based on the cell center. The cell resolutions used for this study in most cases for TreeVaw (Table 5) and watershed segmentation (Table 4) were 0.3 and 1.0 m, respectively.

In many cases it was obvious when the same tree was identified by each program based on spatial location and height. It is also interesting to note that in no case was the same tree identified in the exact same location (Figure 6, Table 13). Again this may be attributed to differences in spatial resolution and precision of measurement, but some may also be attributed to differences in computer algorithms.

Table 13. Comparison of horizontal distance (m) between trees determined to be the same feature. Selection criterion was that the tree was delineated in all four methods (field, FUSION, TreeVaW and watershed segmentation).

Plot/Statistic	Field to Fusion distance	Field to TreeVaW distance	Field to WS Seg. distance	Fusion to TreeVaW distance	Fusion to WS Seg. distance	TreeVaW to WS Seg. distance	Combined	*n*
C110								9
Average	0.99	1.49	1.51	1.04	0.91	0.65	1.10	
SD	0.87	0.96	1.14	0.62	0.41	0.42	0.81	
E200								534
Average	1.66	1.68	1.75	0.48	0.85	0.61	1.17	
SD	1.11	1.08	1.06	0.45	0.43	0.39	0.98	
O16								62
Average	3.02	3.44	3.18	1.50	1.46	0.98	2.26	
SD	2.50	2.30	2.20	1.64	1.63	1.72	2.24	
O69								46
Average	2.76	3.23	3.18	1.43	1.34	1.46	2.23	
SD	1.75	2.97	2.12	2.55	1.87	3.09	2.57	

Table 13. *Cont.*

U8								55
Average	1.59	1.38	1.42	0.70	0.99	0.68	1.13	
SD	1.17	1.21	0.99	0.45	1.58	1.57	1.27	
U13								75
Average	3.21	3.28	3.49	1.41	1.16	1.15	2.28	
SD	2.61	2.62	2.97	1.41	1.30	1.85	2.44	
Total								781
Average	1.97	2.04	2.09	0.73	0.97	0.75	1.42	
SD	1.62	1.73	1.67	1.05	0.95	1.20	1.53	

Field data for plot C110 was collected using GPS, all other plots by total station.

Figure 6. Plot maps of trees used for height comparisons of FUSION, TreeVaW and watershed segmentation matched trees and all field measured trees. Tree locations were measured by GPS in C110 and total station in all others. Plot E200 tree symbols are smaller than others to facilitate point differentiation detail and pattern based on the larger number of trees delineated.

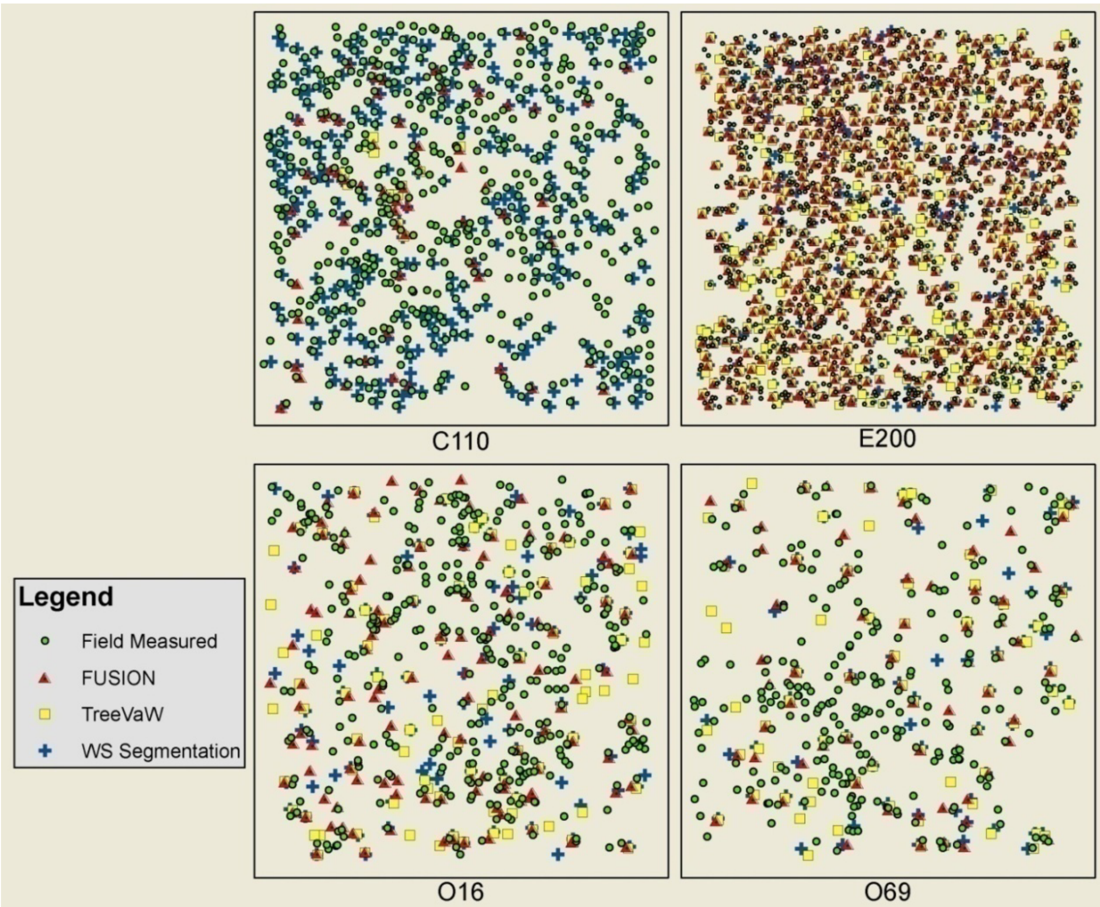

Figure 6. *Cont.*

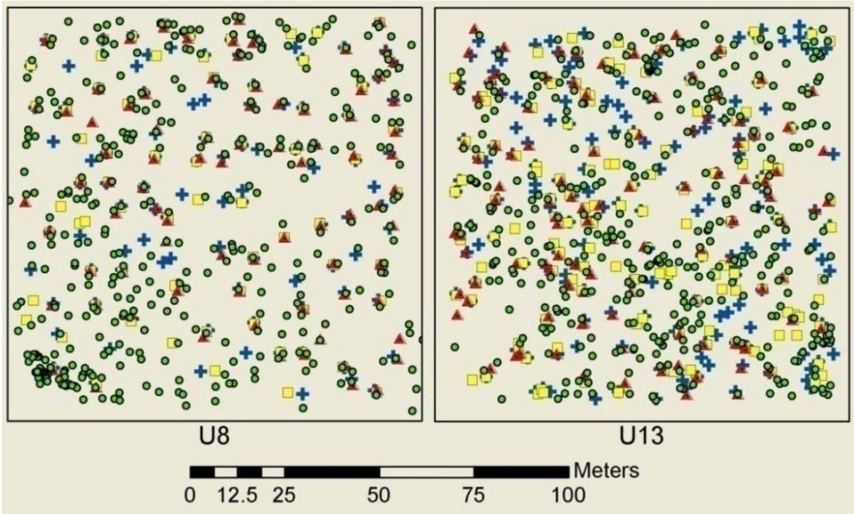

3.5. Biomass Comparison

The TAGB comparison includes a total of all feature to feature comparisons for each plot (Table 14), a comparison of mean TAGB per feature in each plot (Table 15), and a comparison of total TAGB for each plot for each LiDAR extraction method (FUSION, TreeVaW, and watershed segmentation) compared to TAGB estimated from field measurements (Table 16). In comparing model-based estimates to field-based estimates overall, FUSION underestimated TAGB by 25%, TreeVaW underestimated by 31%, and watershed segmentation overestimated by 53% of total weight by kg (Table 14). The watershed segmentation overestimation was primarily due to an extreme overestimation in one plot (U56, 504%). Excluding plot U56, the watershed segmentation method overestimated TAGB by 10%. LiDAR TAGB underestimation occurred in 66% of the plot comparisons (19 of 29) and overestimation occurred in 34% of the comparisons. Nine of the 29 comparisons were within 20% (over or under) of the ground estimations. In five out of six comparisons, FUSION underestimated TAGB. In plot U8, FUSION overestimated by 10%. TreeVaW underestimated TAGB in eight of eleven comparisons. The overestimations occurred in plot C61 (20%), plot U13 (29%), and plot U56 (3%). Watershed segmentation resulted in underestimation in six of eleven plots. The watershed segmentation method overestimations occurred in all plot treatments except clearcut (E200, 25%; O69, 14%; U8, 54%; U13, 35%; U56 504%) (Table 14). The anomaly in plot U56 was due to count and height overestimation of trees over 20 m tall. The field survey resulted in 146 trees over 20 m tall however the watershed segmentation method delineated 665 features over 20 m tall. Average tree height for plot U56 was larger than the field measured data by a factor of four. It was thought that multiple over 20 m tall features were designated where large bigleaf maples occurred, however not enough maples were on this plot to account for such an excess. We evaluated TAGB estimates for plot U56 with TreeVaW for 0.3 m resolution CHM using a 3 × 3 filter and a 0.1 m resolution CHM and 5 × 5 filter to illustrate TAGB differences caused by errors of commission in the 0.1 m CHM. The 0.1 m resolution CHM resulted in a total biomass estimate (743,438 kg/ha) that was nearly five times that of the 0.3 m resolution CHM. The watershed segmentation method resulted in similarly extreme errors of commission in plot U56. We could not determine another explanation for the overestimation.

Table 14. TAGB estimates by plot using BIOPAK. Field measurement data calculated per tree by species. LiDAR calculations by feature based on large Douglas-fir (DBH ≥ 0.13 m) and small Douglas-fir (DBH < 0.13 m).

Plot	Method	Average Tree Height (m)	Min. Tree Height (m)	Max Tree Height (m)	Tree Biomass kg/ha	Shrub Biomass kg/ha	Biomass Total kg/ha	Percent of Field measured
C20	Field Measured	1.06	0.02	35.00	553	58	611	
	FUSION			NOT MEASURED				
	TreeVaW	1.20	0.03	8.66			442	72.37
	WS Segmentation	0.87	0.35	9.05			478	78.19
C27	Field Measured	1.04	0.54	8.63	357	59	416	
	FUSION			NOT MEASURED				
	TreeVaW	2.50	1.21	9.36			289	69.49
	WS Segmentation	0.53	0.19	20.65			345	83.03
C61	Field Measured	1.70	0.32	44.45	16295	0	16,295	
	FUSION			NOT MEASURED				
	TreeVaW	15.03	1.22	41.55			19,479	119.54
	WS Segmentation	1.68	0.35	41.85			4,731	29.03
C110	Field Measured	1.87	0.32	9.40	987	240	1,227	
	FUSION	2.06	0.36	9.69			333	27.12
	TreeVaW	3.16	1.37	9.53			612	49.85
	WS Segmentation	0.97	0.35	9.58			457	37.28
E200	Field Measured	12.52	1.04	18.31	83070	266	83,336	
	FUSION	13.67	6.50	17.40			69,006	82.80
	TreeVaW	13.02	5.69	17.34			75,700	90.84
	WS Segmentation	12.43	1.07	17.34			103,913	124.69
E412	Field Measured	6.56	1.21	21.37	15592	239	15,831	
	FUSION			NOT MEASURED				
	TreeVaW	4.69	1.76	20.56			6,993	44.17
	WS Segmentation	4.45	0.90	20.56			12,883	81.38

Table 14. *Cont.*

Plot	Method	Average Tree Height (m)	Min Tree Height (m)	Max Tree Height (m)	Tree Biomass kg Per Hectare	Shrub Biomass kg Per Hectare	Biomass Total kg/ha	Percent of Field Measured
O16	Field Measured	18.86	1.05	64.70	472,976	1,868	474,844	
	FUSION	31.16	4.02	63.88			293,328	61.77
	TreeVaW	19.46	3.02	63.57			197,288	41.55
	WS Segmentation	35.15	1.38	63.62			416,444	87.70
O69	Field Measured	20.22	2.05	69.71	366,511	1,755	368,266	
	FUSION	43.94	1.14	68.70			261,929	71.12
	TreeVaW	19.81	2.75	68.20			216,549	58.80
	WS Segmentation	31.49	1.13	31.49			421,644	114.49
U8	Field Measured	18.00	1.10	57.88	215,013	1,722	216,735	
	FUSION	45.65	16.07	54.03			238,278	109.94
	TreeVaW	25.97	1.95	53.91			164,559	75.93
	WS Segmentation	35.56	0.97	53.79			332,918	153.61
U13	Field Measured	6.67	0.56	52.60	141,586	279	141,865	
	FUSION	16.66	1.54	53.08			97,340	68.61
	TreeVaW	10.53	3.36	52.78			183,065	129.04
	WS Segmentation	16.18	0.92	52.87			191,971	135.32
U56	Field Measured	6.66	1.00	42.36	146,791	208	146,999	
	FUSION				NOT MEASURED			
	TreeVaW 0.3/3 × 3	15.18	1.71	42.52			151,046	102.75
	TreeVaW 0.1/5 × 5	20.92	2.56	42.52			743,438	505.74
	WS Segmentation	26.69	0.91	42.52			760,674	503.60
						Study Totals		
						Field Measured	1,466,425	
						FUSION Total	960,214	74.65
						TreeVaW Total	1,016,022	69.29
						WS Segmentation	2,246,459	153.19

Plot characteristics in this study were highly variable. The variability in the LiDAR TAGB estimation results are a manifestation of the field variability. These results make it difficult to consistently predict TAGB per plot however we noted that many TAGB estimates were within 10 to 20% of the field based estimates. If plot U56 watershed segmentation TAGB results are removed, the watershed segmentation overall TAGB estimation was 13% over field estimates, thus the overall estimation was within just over 30% or better considering the three delineation methods. These overall results indicate promise in using LiDAR for broad, forest level TAGB estimation.

Using a Welch modified t-test to examine the differences in mean feature (tree/shrub) TAGB by plot (Table 15), statistically significant differences ($p \leq 0.03$) were observed in all but one plot and in 17 of 28 LiDAR extraction methods. Potentially equal TAGB means could not be ruled out in plot C20. FUSION overestimated mean TAGB in all plots, and in 66% of the plots (E200, O69, U8, and U13) this overestimation was statistically significant noting that these were all plots with significant canopy cover. Plot O16 also had significant canopy cover, however 58% of the trees were larger than 10 m tall, and of the 32% below 10 m tall, there were very few seedlings. TreeVaW displayed statistically significant differences in 8 of 11 plots (p-values ≤ 0.03). The three plots that did not display significant differences were C20, O69, and U13 and were all within 30% of the field measured TAGB estimate. The watershed segmentation method had inconclusive results in the clearcut plots, but in all other comparisons to field based TAGB estimation resulted in statistically significant differences.

Table 15. Probability that LiDAR (L) based feature mean TAGB estimates by plot are equal to field (F) measurement estimates.

Plot	Avg Field Biomass (kg)	Avg LiDAR Biomass (kg)	(µ F bio) − (µ L bio) 95% CI *	df	t	*p*-value
C20						
FUSION			NOT MEASURED			
TreeVaW	2.40	2.06	3.01	704	0.21	0.58
WS Seg.	2.40	0.57	4.48	695	1.13	0.87
C27						
FUSION			NOT MEASURED			
TreeVaW	0.63	2.51	−1.31	134	−5.47	<0.01
WS Seg.	0.63	0.53	0.27	816	0.90	0.81
C61						
FUSION			NOT MEASURED			
TreeVaW	30.34	105.86	−26.66	655	−2.53	0.01
WS Seg.	30.34	7.49	68.84	540	0.82	0.79
C110						
FUSION	1.73	1.81	0.25	323	−0.41	0.34
TreeVaW	1.73	3.56	−1.35	224	−6.34	<0.01
WS Seg.	1.73	0.74	1.19	947	8.13	1.00
E200						
FUSION	87.81	105.03	−22.29 − (−13.15)	1,376	−8.29	<0.01
TreeVaW	87.81	107.53	−24.34 − (−15.09)	1,638	−8.36	<0.01
WS Seg.	87.81	97.38	−13.81 − (−5.34)	1,578	−4.44	<0.01
E412						
FUSION			NOT MEASURED			
TreeVaW	16.78	6.66	9.04 − 11.20	1,945	18.37	<0.01

Table 15. *Cont.*

WS Seg.	16.78	13.46	1.82 − 4.82	1,589	4.35	<0.01
O16						
FUSION	1,288.76	1,585.56	−675.48 − 81.88	504	−1.54	0.12
TreeVaW	1,288.76	904.99	30.68 − 736.87	581	2.13	0.03
WS Seg.	1,288.76	1,983.07	−1054.76 − (−333.84)	566	−3.78	<0.01
O69						
FUSION	1,415.10	3,045.69	−2182.08 − 1079.08	201	−5.83	<0.01
TreeVaW	1,415.10	1,099.23	−118.14 − 749.87	448	1.43	0.15
WS Seg.	1,415.10	1,899.30	−909.69 − (−58.70)	457	−2.24	0.03
U8						
FUSION	584.27	2,707.71	−2302.89 − (−1943.97)	202	−23.33	<0.01
TreeVaW	584.27	1,337.88	−1027.90 − (−479.31)	170	−5.42	<0.01
WS Seg.	584.27	1,743.02	−1348.45 − (−969.05)	374	−12.01	<0.01
U13						
FUSION	284.31	662.18	−579.28 − (−176.45)	218	−3.70	<0.01
TreeVaW	284.31	325.81	−173.56 − 90.55	658	−0.62	0.54
WS Seg.	284.31	615.29	−466.54 − (195.42)	689	−4.79	<0.01
U56						
FUSION			NOT MEASURED			
TreeVaW	117.53	547.27	−523.53 − (−335.96)	300	−9.02	<0.01
WS Seg.	117.53	923.15	−847.36 − (−763.88)	1,273	−37.87	<0.01

* Clearcut plots are one-sided *p* values.

Consolidating features (trees/shrubs) together from all plots and determining a feature average resulted in statistically significant differences ($p < 0.01$) between each LiDAR extraction method compared to field measurements (Table 16). All LiDAR TAGB feature average estimates were larger than field estimates. When combining and analyzing plot TAGB, statistical significance was inconclusive in all cases. Plot average TAGB estimated by LiDAR was less than field measurements in both FUSION and TreeVaW but was greater for the watershed segmentation results.

Table 16. Probability that LiDAR (L) based mean TAGB estimates for all features combined are equal to field (F) measurement estimates.

Plot	Avg Field Biomass (kg)	Avg LiDAR Biomass (kg)	(μ F bio) − (μ L bio) 95% CI	df	t-stat	*p*-value
Average Feature						
FUSION Plots	425.44	712.85	−376.38 − (−198.45)	2,751	−6.33	<0.01
TreeVaW Plots	209.41	261.60	−87.47 − (−16.34)	8,300	−2.84	<0.01
WS Seg Plots.	209.41	345.29	−166.90 − (−105.28)	13,308	−8.75	<0.01
Average by Plot						
FUSION Plots	214,379	160,035	−145,189.80 − 253,876.60	9	0.61	0.55
TreeVaW Plots	133,312	84,046	−68,142.39 − 166,673.07	15	0.95	0.38
WS Seg. Plots.	133,312	204,223	−260,773.90 − 118,950.2	17	−0.79	0.44

4. Discussion

We presented a comparison of FUSION, TreeVaW, and watershed segmentation tree extraction methods in clearcut, even-age, uneven-age, and old growth forest plots using an extensive tree inventory. Our examination and comparison of metrics from the extraction methods included tree height and spatial position. In addition, we compared resulting TAGB estimates from the tree extraction methods.

We reported LiDAR tree height errors using FUSION, TreeVaW, and watershed segmentation extraction methods in our study plots. These errors are generally consistent with those reported in other studies of LiDAR height measurements in various forest conditions compared to field measurements, albeit somewhat higher than some in old growth plot O69 and uneven-aged plot U8 [10,38-40]. To illustrate the complexity in measuring individual trees with LiDAR, many factors influencing the accuracy of LiDAR forest measurement are reviewed below. Some of the key factors that impact LiDAR tree height measurement include survey control, location the LiDAR pulse(s) strike the tree, base measurement datum, differentiating individual trees, position of the tree within the canopy, and use of a raster CHM versus the LiDAR point cloud.

The vendor provided resolution and accuracy summary for this study stated a point resolution specification of ≥8 points/m^2 and an achieved resolution of 10 points/m^2, and a vertical accuracy of better than 0.13 m. This accuracy is based on measurements made in perfect LiDAR ground conditions, such as those found on paved road surfaces with no vertical obstruction. The resolution and accuracy deteriorates markedly with variation in natural terrain conditions including forest canopy, understory vegetation, small scale topography, and other environmental conditions.

Field measurements are subject to systematic and random error propagation. The field survey crew was trained in proper procedures and the design of proper protocols prevented many potential errors. However due to the scope of this study, it is wrought with a myriad of potential accidental errors. The field survey measured thousands of features, thus error is likely to have occurred periodically in tree height measurement with a laser range finder (both systematic and accidental). Laser range finders are known to introduce height error, however we used one that has been shown to have the highest accuracy in comparison to other commonly used models [36].

Where and how many LiDAR pulses strike and reflect off the tree impacts tree identification and measurement. In conifer species the odds of a pulse striking a single, very thin apex are low. These odds decrease further when the tree occurs below the primary canopy where pulses that might strike the tree are intercepted by the upper canopy. In every method of tree extraction used in this study the number of pulses hitting the tree impacts identification and canopy dimension measurements. Without an adequate number of pulses striking a tree in FUSION, tree identification was difficult in both dense and clearcut forest plots. In dense plots, upper tree identification was relatively easy based on the unique shape and canopy of each tree, however, as smaller trees were shrouded by larger ones, tree identification was difficult at best. Manually identifying a three dimensional array of dots (the LiDAR point cloud) that belong to a single tree is a tedious process. Differentiating small trees in a clearcut where overstory trees are not a factor was also very difficult. This is strictly a result of LiDAR resolution. Theoretically one would think that a pulse rate of 8–10 pulses per m^2 would be enough to enable the identification of small conifers whose crown is approximately 1 m^2. However, due to the sparseness of young conifer foliage, often only one or two LiDAR points struck a tree, which made identification difficult to impossible.

TreeVaW and watershed segmentation both rely on a CHM for tree identification and measurement. If points are generated from trees existing below the primary canopy, these points will be eliminated in rendering the CHM surface, thus the tree that exists in the field will be removed from the model. In creating the CHM, we also experimented with raster interpolation resolution. In both models, the 0.1 m resolution CHMs resulted in extreme commission errors (Tables 7 and 8). This is likely due to false canopy peaks introduced where branch height variation caused algorithm calculation error. The software determined a separate tree location based on a LiDAR branch peak returns surrounded by lower height LiDAR pulse returns, when in fact many returns were associated with a single tree. This consistently occurred in commission errors caused by returns from broadleaf trees where upward facing branches along outward extending large branches caused the algorithm to falsely delineate individual trees. Watershed segmentation results found that in 8 of 11 plots the 1m resolution CHM best matched the field measured results. Since the algorithm relies on an inverted CHM to find sills/pits in the raster elevations and in many cases tree tops are 1m apart, it stands to reason that 1m resolution raster cells would avoid errors of commission caused by branch peaks associated within the same tree. TreeVaW's algorithm appeared to have difficulty finding small trees, even in the clearcut plots where only small trees existed. Excluding the 0.1 m resolution CHM issues addressed above, the differences in resolution appears to be mostly related errors of omission associated with small trees.

All LiDAR tree height measurement methods rely on some form of ground surface elevation model. In this study, all utilized methods relied on a vendor provided DEM. We chose to use this DEM instead of creating our own based on the vendor having the expertise and software necessary to separate ground points from non-ground points such as understory vegetation, stumps, and slash. In certain circumstances, when conducting the ground survey, it was obvious that a LiDAR pulse would not reach the ground surface. Examples of this are dense blackberry, poison oak, and Oregon grape thickets. It is questionable if computer software or an analyst could always identify these features. Even if positively identified, many thickets in this study occupied 100 m^2 or more. Interpolation of the ground surface under this vegetation likely introduced error in the DEM.

What level of vertical accuracy is good enough for a tree height measurement? What is the impact if LiDAR height estimation is off by 1 m? If the estimate is under or over from a timber management perspective, then tree volume estimates will be wrong. On the other hand, a loss of some of the tree top is expected in felling operations. For illustrative purposes and from a biomass estimation perspective, we calculated the impact of height errors based on Douglas-fir TAGB in small trees of the same height used in this study (Table 17). These calculations are based on small Douglas-fir TAGB equations for a single tree and multiplied by the number of trees. This small tree equation was used to represent the approximate size of the top of a tree. Volume estimates are highly variable based on the height of the tree used in allometric equations, and the allometric equation itself, thus the calculations are conservative. Ground truth confirmation would likely be prudent in economic decisions involving LiDAR volume/biomass estimation.

Table 17. TAGB error estimate based on LiDAR height error.

	1.0 m error (kg)	1.5 m error (kg)	2.0 m error (kg)
Single Tree	0.68	1.07	1.62
100 Trees	67.85	106.58	161.67
500 Trees	339.25	532.91	808.35
1,000 Trees	678.50	1,065.83	1,616.71

We found that there are three main factors that influence the accuracy of LiDAR forest TAGB estimates: feature (tree/shrub) count, feature height, and species identification. In this study, the factor that contributed the most to biomass calculation differences was the tree count. All three algorithms did well at detecting large trees however watershed segmentation appears to detect small trees better than TreeVaW or FUSION. This study illustrates that the effectiveness of using LiDAR with the protocols we used for forest measurement has its limitations. Based on this research and previous studies, further investigation is warranted and development of regional protocols could result in LiDAR becoming a very effective forest measurement tool for volume and biomass estimates. Clearly, this and previous studies have demonstrated that large trees or even-age stands with consistent species and size can be measured using LiDAR with relatively accurate results. However, measuring all trees and shrubs at the stand or forest level for purposes of estimating TAGB is not necessarily accurate compared to field-based estimates. Detecting and measuring small and understory vegetation would likely improve with increased LiDAR resolution (greater pulse density) and warrants further investigation. We also found that the cell resolution of the CHM impacted tree extraction results in TreeVaW and watershed segmentation. Further research is recommended to determine one ideal CHM resolution for stand level tree extraction and biomass estimation, or a potential solution is to use different resolutions per stand treatment. The use of the LiDAR point clouds enable the measurement of all features vertically throughout the canopy structure, however the manual method of feature extraction in FUSION is tedious and slow relative to automated methods, but automated methods used in this study were limited by the CHM. An automated method of feature extraction using point clouds may be a solution to improved measurement accuracy. This study was also limited in estimating TAGB because we did not differentiate species in LiDAR estimations. One method to identify species is to use other imagery, e.g., multispectral aerial photographs or satellite imagery in conjunction with LiDAR. One recommendation is that, if budgets permit, aerial photographs should be taken simultaneously with the LiDAR. The LiDAR system used in this study also acquired return intensity values, which we feel can be used to differentiate conifer from deciduous species, and will be further investigated to improve biomass estimates. Finally, biomass estimates vary widely in their accuracy when relying on allometric equations. Based on many site specific factors and age classes, predicting TAGB developed from different sites and ages can raise debate [37]. A great deal more variation in biomass equation prediction exists than many realize. Variation in equations is likely by at least ±25–50% (Harmon, M. Personal communication, 30 November 2010).

References

1. Falkowski, M.J.; Smith, A.M.S.; Gessler, P.E.; Hudak, A.T.; Vierling, L.A.; Evans, J.S. The influence of conifer forest canopy cover on the accuracy of two individual tree measurement algorithms using lidar data. *Canad. J. Remote Sens.* **2008**, *34*, S1-S13.
2. Hyyppa, J.; Hyyppa, H.; Litkey, P.; Yu, X.; Haggren, H.; Ronnholm, P.; Pyysalo, U.; Pitkanen, J.; Maltamo, M. Algorithms and Methods of Airborne Laser Scanning for Forest Measurements. In *Proceedings of the ISPRS Working Group VIII/2 "Laser-Scanners for Forest and Landscape Assessment"*, Freiburg, Germany, 3–6 October 2004; In *IAPRS*; 2004; Volume 36, pp. 82-89.
3. Bortolot, Z.J.; Wynne, R.H. Estimating forest biomass using small footprint lidar data: An individual tree-based approach that incorporates training data. *ISPRS J. Photogramm.* **2005**, *59*, 342-360.
4. Lucas, R.M.; Lee, A.C.; Bunting, P.J. Retrieving forest biomass through integration of casi and lidar data. *Int. J. Remote Sens.* **2008**, *29*, 1553-1577.
5. Zhou, X.; Hemstrom, M.A. *Estimating Aboveground Tree Biomass on Forest Land in the Pacific Northwest: A Comparison of Approaches*; PNW-RP-584; USDA: Portland, OR, USA, November 2009; pp. 1-18.
6. Sessa, R. *Assessment of the Status of the Development of the Standards for the Terrestrial Essential Climate Variables: Biomass*; GTOS, FAO: Rome, Italy, 25 May 2009; pp. 1-18.
7. Popescu, S.C.; Randolph, H.W.; John, A.S. Fusion of small-footprint lidar and multispectral data to estimate plot- level volume and biomass in deciduous and pine forests in virginia, USA. *Forest Sci.* **2004**, *50*, 551-565.
8. Lim, K.; Treitz, P.; Wulder, M.; St-Onge, B.; Flood, M. Lidar remote sensing of forest structure. *Progr. Phys. Geogr.* **2003**, *27*, 88-106.
9. Andersen, H.-E.; Reutebuch, S.E.; McGaughey, R.J. A rigorous assessment of tree height measurements obtained using airborne lidar and conventional field methods. *Can. J. Remote Sens.* **2006**, *32*, 355-366.
10. Husch, B.; Miller, C.I.; Beers, T. *Forest Mensuration*, 3rd ed.; John Wiley and Sons: New York, NY, USA, 1982; p. 402.
11. Anderson, E.S.; Thompson, J.A.; Crouse, D.A.; Austin, R.E. Horizontal resolution and data density effects on remotely sensed lidar-based dem. *Geoderma* **2006**, *132*, 406-415.
12. Popescu, S.C.; Wynne, R.H.; Nelson, R.F. Estimating plot-level tree heights with lidar: Local filtering with a canopy-height based variable window size. *Comput. Electron. Agric.* **2002**, *37*, 71-95.
13. Lovell, J.L.; Jupp, D.L.B.; Newnham, G.J.; Coops, N.C.; Culvenor, D.S. Simulation study for finding optimal lidar acquisition parameters for forest height retrieval. *Forest Ecol. Manage.* **2005**, *214*, 398-412.
14. Kraus, K.; Pfeifer, N. Determination of terrain models in wooded areas with airborne laser scanner data. *ISPRS J. Photogramm.* **1998**, *53*, 193-203.
15. Andersen, H.-E.; McGaughey, R.J.; Reutebuch, S.E. Estimating forest canopy fuel parameters using lidar data. *Remote Sens. Environ.* **2005**, *94*, 441-449.

16. SAF. The Dictionary of Forestry. Available online: http://dictionaryofforestry.org/ (accessed on 29 August 2010).
17. Williams, M.S.; Schreuder, H.T. Guidelines for choosing volume equations in the presence of measurement error in height. *Can. J. Forest Res.* **2000**, *30*, 306-310.
18. Næsset, E.; Bjerknes, K.-O. Estimating tree heights and number of stems in young forest stands using airborne laser scanner data. *Remote Sens. Environ.* **2001**, *78*, 328-340.
19. Brandtberg, T.; Warner, T.A.; Landenberger, R.E.; McGraw, J.B. Detection and analysis of individual leaf-off tree crowns in small footprint, high sampling density lidar data from the eastern deciduous forest in north america. *Remote Sens. Environ.* **2003**, *85*, 290-303.
20. Hyyppa, J.; Hyyppa, H.; Leckie, D.; Gougeon, F.; Yu, X.; Maltamo, M. Review of methods of small-footprint airborne laser scanning for extracting forest inventory data in boreal forests. *Int. J. Remote Sens.* **2008**, *29*, 1339-1366.
21. McGaughey, R.J.; Carson, W.W.; Reutebuch, S.E. Direct Measurement of Individual Tree Characteristics from Lidar Data. In *Proceedings of the 2004 Annual ASPRS Conference*, Denver, CO, USA, 23–28 May 2004.
22. Goerndt, M.E. Comparison and Analysis of Small Area Estimation Methods for Improving Estimates of Selected Forest Attributes. Ph.D. Dissertation, Oregon State University, Corvallis, OR, USA, 2010.
23. Andersen, H.-E. Using airborne light detection and ranging (lidar) to characterize forest stand condition on the kenai peninsula of alaska. *Western J. Appl. Forest.* **2009**, *24*, 95-102.
24. Goerndt, M.E.; Monleon, V.J.; Temesgen, H. Relating forest attributes with area- and tree-based light detection and ranging metrics for western Oregon. *Soc. Amer. Forest.* **2010**, *25*, 105-111.
25. Popescu, S.C.; Wynne, R.H. Seeing the trees in the forest: Using lidar and multispectral data fusion with local filtering and variable window size for estimating tree height. *Photogramm. Eng. Remote Sensing* **2004**, *70*, 589-604.
26. Jensen, J.R. *Introductory Digital Image Processing*, 2nd ed.; Prentice Hall: Upper Saddle River, NJ, USA, 1996.
27. Kini, A.U.; Popescu, S.C. TreeVaW: A Versatile Tool for Analyzing Forest Canopy LiDAR Data—A Preview with an Eye towards Future. In *Proceedings of the ASPRS 2004 Fall Conference*, Kansas City, MO, USA, 12–16 September 2004; pp. 1-10.
28. McGaughey, R. *Fusion/LDV: Software for Lidar Data Analysis and Visualization*; USDA Forest Service, Pacific Northwest Research Station: Portland, OR, USA, 2007.
29. Van Sickle, J. *GPS for Land Surveyors*, 3rd ed.; CRC Press, Taylor & Francis Group: Boca Raton, FL, USA, 2008; p. 338.
30. Trimble. *Terrasync Software Reference Manual*; Version 2.60; Trimble Navigation Limited: Westminster, CO, USA, 2006; pp. 1-248.
31. Watershed Sciences. *Lidar Remote Sensing Data Collection: Mcdonald-Dunn Research Forest*; Watershed Sciences Inc.: Corvallis, OR, USA, August 2008; p. 20.
32. Popescu, S.C. *TreeVaw: Tree Variable Window*; Spatial Sciences Laboratory, Texas A&M University: College Station, TX, USA. Available online: http://ssl.tamu.edu/personnel/s_popescu/TreeVaW/download.htm (accessed on 11 December 2010).

33. USDA Forest Service. *Introduction to Fusion Launch Page*; Remote Sensing Applications Center: Salt Lake City, UT, USA. Available online: www.fs.fed.us/eng/rsac/fusion/index.html (accessed on 15 January 2008).
34. Means, J.E.; Hanson, H.A.; Koerper, G.J.; Alaback, P.B.; Klopsch, M.W. *Software for Computing Plant Biomass-Biopak Users Guide*; PNW-GTR-340; United States Department of Agriculture Forest Service: Portland, OR, USA, August 1994; p. 194.
35. Jennings, S.; Brown, N.; Sheil, D. Assessing forest canopies and understorey illumination: Canopy closure, canopy cover and other measures. *Forestry* **1999**, *72*, 59-74.
36. Wing, M.G.; Solmie, D.; Kellogg, L. Comparing digital range finders for forestry applications. *J. Forest.* **2004**, *102*, 16-20.
37. St. Clair, J.B. Family differences in equations for predicting biomass and leaf area in Douglas-fir (pseudotsuga menziesii var. Menziesii). *Forest Sci.* **1993**, *39*, 743-756.
38. Næsset, E.; Økland, T. Estimating tree height and tree crown properties using airborne scanning laser in a boreal nature reserve. *Remote Sens. Environ.* **2002**, *79*, 105-115.
39. Brandtberg, T.; Warner, T.A.; Landenberger, R.E.; McGraw, J.B. Detection and analysis of individual leaf-off tree crowns in small footprint, high sampling density lidar data from the eastern deciduous forest in North America. *Remote Sens. Environ.* **2003**, *85*, 290-303.
40. Gaveau, D.L.A.; Hill, R.A. Quantifying canopy height underestimation by laser pulse penetration in small-footprint airborne laser scanning data. *Can. J. Remote Sens*. **2003**, *29*, 650-657.